

Peatland Initiation, Carbon Accumulation, and 2 ka Depth in the James Bay Lowland and Adjacent Regions

Authors: Holmquist, James R., MacDonald, Glen M., and Gallego-Sala, Angela

Source: Arctic, Antarctic, and Alpine Research, 46(1) : 19-39

Published By: Institute of Arctic and Alpine Research (INSTAAR),
University of Colorado

URL: <https://doi.org/10.1657/1938-4246-46.1.19>

BioOne Complete (complete.BioOne.org) is a full-text database of 200 subscribed and open-access titles in the biological, ecological, and environmental sciences published by nonprofit societies, associations, museums, institutions, and presses.

Your use of this PDF, the BioOne Complete website, and all posted and associated content indicates your acceptance of BioOne's Terms of Use, available at www.bioone.org/terms-of-use.

Usage of BioOne Complete content is strictly limited to personal, educational, and non - commercial use. Commercial inquiries or rights and permissions requests should be directed to the individual publisher as copyright holder.

BioOne sees sustainable scholarly publishing as an inherently collaborative enterprise connecting authors, nonprofit publishers, academic institutions, research libraries, and research funders in the common goal of maximizing access to critical research.

Peatland Initiation, Carbon Accumulation, and 2 ka Depth in the James Bay Lowland and Adjacent Regions

James R. Holmquist*

Glen M. MacDonald† and

Angela Gallego-Sala‡

*Corresponding author: Department of Ecology and Evolutionary Biology, UCLA, Hershey Hall, Box 957246, Los Angeles, California 90095-7246, U.S.A., jamesholmquist@ucla.edu

†Institute of the Environment and Sustainability and Department of Ecology and Evolutionary Biology, UCLA, La Kretz Hall, Suite 300B, Los Angeles, California 90095-1496, U.S.A.

‡Department of Geography, University of Exeter, Amory Building, Office 436, Rennes Drive, Exeter, EX4 4RJ, U.K.

Abstract

Peatlands surrounding Hudson and James Bays form the second largest peatland complex in the world and contain major stores of soil carbon (C). This study utilized a transect of eight ombrotrophic peat cores from remote regions of central and northern Ontario to quantify the magnitude and rate of C accumulation since peatland initiation and for the past 2000 calendar years before present (2 ka). These new data were supplemented by 17 millennially resolved chronologies from a literature review covering the Boreal Shield, Hudson Plains, and Taiga Shield bordering Hudson and James Bays. Peatlands initiated in central and northern Ontario by 7.8 ka following deglaciation and isostatic emergence of northern areas to above sea level. Total C accumulated since inception averaged $109.7 \pm$ (std. dev.) 36.2 kg C m^{-2} . Approximately 40% of total soil C has accumulated since 2 ka at an average apparent rate of $20.2 \pm 6.9 \text{ g C m}^{-2} \text{ yr}^{-1}$. The 2 ka depths correlate significantly and positively with modern gridded climate estimates for mean annual precipitation, mean annual air temperature, growing degree-days $> 0^\circ \text{C}$, and photosynthetically active radiation integrated over days $> 0^\circ \text{C}$. There are significantly shallower depths in permafrost peatlands. Vertical peat accumulation was likely constrained by temperature, growing season length, and photosynthetically active radiation over the last 2 ka in the Hudson Bay Lowlands and surrounding regions.

DOI: <http://dx.doi.org/10.1657/1938-4246-46.1.19>

Introduction

Northern peatlands have acted as a terrestrial carbon (C) sink since the end of the last glacial maximum (MacDonald et al., 2006) and are estimated to have stored over 30% of global soil C in only 2–3% of the earth's land surface (Gorham, 1991; Turetsky et al., 2002; Bridgman et al., 2006; Yu et al., 2009). Short growing seasons, low mean annual temperatures, poorly drained land, and complex ecohydrological processes create conditions where net ecosystem productivity can remain positive (Clymo, 1984; van Breemen, 1995; Blodau, 2002; Dise, 2009; Yu et al., 2009). This positive net ecosystem productivity may increase, decrease, or reverse due to projected anthropogenic climate change (Moore and Knowles, 1989; Davidson and Janssens, 2006; Tarnocai, 2006; Beilman et al., 2009; Loisel et al., 2012). Therefore, it is important to understand peatland C storage so that soil C is accounted for in international climate change agreements (Roulet, 2000; Waddington et al., 2009; Dunn and Freeman, 2011) and in improving vegetation, soil, and climate models (Wania et al., 2009a, 2009b), and in evaluating possible mitigation options for projected climate change (Carlson et al., 2010; Freeman et al., 2012).

At present, peatlands store 270 to 450 Pg of C (Gorham, 1991). Global reports state that northern latitude peatlands store an average of 2.3 m depth times 130 kg C m^{-2} of peat (Gorham, 1991). Long-term net rates of C accumulation in Canadian peatlands typically range from 10 to $35 \text{ g C m}^{-2} \text{ yr}^{-1}$ (Ovenden, 1990; Gorham et al., 2003). These figures are comparable to other large peatland complexes in the West Siberian Lowlands (WSL), which vary from 5.4 to $35.9 \text{ g C m}^{-2} \text{ yr}^{-1}$ (Beilman et al., 2009), as well as various other North American sites. Other North American sites range from 16 to $80 \text{ g C m}^{-2} \text{ yr}^{-1}$ (Gorham et al., 2003), approximately 8 to $40 \text{ g C m}^{-2} \text{ yr}^{-1}$ if we assume a ratio of 0.5 g C for every 1 g peat (Turunen et al., 2002). Due to C storage, peatlands are estimated

to have had a net global cooling effect of -0.2 to -0.5 W m^{-2} since their initiation, after an initial net warming effect of approximately 0.1 W m^{-2} due to CO_2 and CH_4 emissions (Frolking and Roulet, 2007).

This paper focuses on the Boreal Shield and the Hudson Plains of central and northern Ontario, and it synthesizes data from the Boreal Shield, Hudson Plains, and Taiga Shield bordering the Hudson and James Bays. We present data on the initiation, development, and patterns of C storage in ombrotrophic peatlands during the course of the Holocene, and since 2000 cal. yr BP (2 ka). Although the Arctic and subarctic have experienced variation in climatic conditions over the past 2000 years, this time period represents the period of the Holocene during which natural radiative forcing, boundary conditions, and Arctic climate are most similar to the present (Kaufman et al., 2009). Data on peatland depth can be useful to make baseline estimates of peat production relative to decay and the potential impacts of climate change (Beilman et al., 2009).

Precipitation and surface moisture may be important drivers of peat accumulation in *Sphagnum* bogs. *Sphagnum* mosses do not have stomata and cannot regulate water loss during CO_2 exchange, making them vulnerable to large shifts in surface moisture (Loisel et al., 2012). Effective moisture has been found to be a significant driver of *Sphagnum* growth in some continental sites (Loisel et al., 2012). However, in a review of North American peat accumulation, precipitation was found to be significantly, but inversely, correlated with peat depth and the rate of accumulation (Gorham et al., 2003). There is also some evidence that *Sphagnum* bogs can regulate their own water table depth because of their complex structure and ecohydrology; therefore they may not be sensitive to precipitation-related water stress within their ecological limits (Laiho, 2006; Dise, 2009). This internal feedback relationship

has been included in many different peatland development models (Clymo, 1984; Belyea and Baird, 2006; Eppinga et al., 2009; Froelking et al., 2010).

Growing season length and thermal characteristics such as air temperature are possible important drivers of *Sphagnum* growth and C accumulation. *Sphagnum* growth rate increases with temperature (Gunnarsson, 2005; Breeuwer et al., 2008). *Sphagnum* productivity has also been globally linked to photosynthetically active radiation, and growing season length (Loisel et al., 2012). Studies have also observed significant, positive correlations worldwide between mean growing degree-days above 0 °C (GDD_0) and rates of peat accumulation (Clymo et al., 1998). As with GDD_0 , photosynthetically active radiation integrated over the growing season (PAR_0) was also shown to be a driver of the rate of post-1 ka apparent C accumulation in a global peatland database (Charman et al., 2013). In an analysis of a widespread network of *Sphagnum* cores in the WSL, the depths of 2 ka peat correlate significantly and positively with mean annual air temperature (MAAT; Beilman et al., 2009). In the WSL, 2 ka depths are also significantly shallower if permafrost is present, suggesting productivity, rather than low decomposition rates, may exercise greater control on peat accumulation at these sites (Beilman et al., 2009).

The peatlands surrounding Hudson and James Bays in Quebec, Ontario, and Manitoba in Canada (Figs. 1 and 2), are second to the WSL as the largest continuous peatland complex in the world (Riley, 2005, 2011). Despite the importance of this

area to global C cycling, only a few studies have estimated average apparent rate of C accumulation over the broad regions of northern Ontario (O'Reilly, 2011; Bunbury et al., 2012), mainly due to inaccessibility by surface transport. In addition to this, no studies have synthesized current patterns, or analyzed connections between peat accumulation and climate over the entire area surrounding the Hudson and James Bays.

This study examines the rates and magnitudes of Holocene and post-2 ka peat and C accumulation in central and northern Ontario based on new data. The study also investigates the relationship between C accumulation and climate based on this new information, and synthesizes existing studies. Radiocarbon (^{14}C)-based estimates of peatland initiation; timing; estimates of average Holocene, post-2 ka, and pre-2 ka apparent rate of C accumulation; and Holocene, post-2 ka, and pre-2 ka C mass totals are presented for eight previously undescribed ombrotrophic peatlands in Ontario (Fig. 1; Table 1). These data are combined with an analysis of 17 other cores from ombrotrophic peat sites from three ecozones surrounding the Hudson and James Bays, which have ^{14}C chronologies of approximately millennial resolution (Dredge and Mott, 2003; Glaser et al., 2004; Arlen-Pouliot and Bhiry, 2005; Kuhry, 2008; Beaulieu-Audy et al., 2009; Sannel and Kuhry, 2009; Loisel and Garneau, 2010; van Bellen et al., 2011; Bunbury et al., 2012). The analysis is used to determine if rates and magnitudes of accumulation at the new sites are representative of 2 ka peat depth, and to gauge the wider effects of climate on 2 ka peat depth.

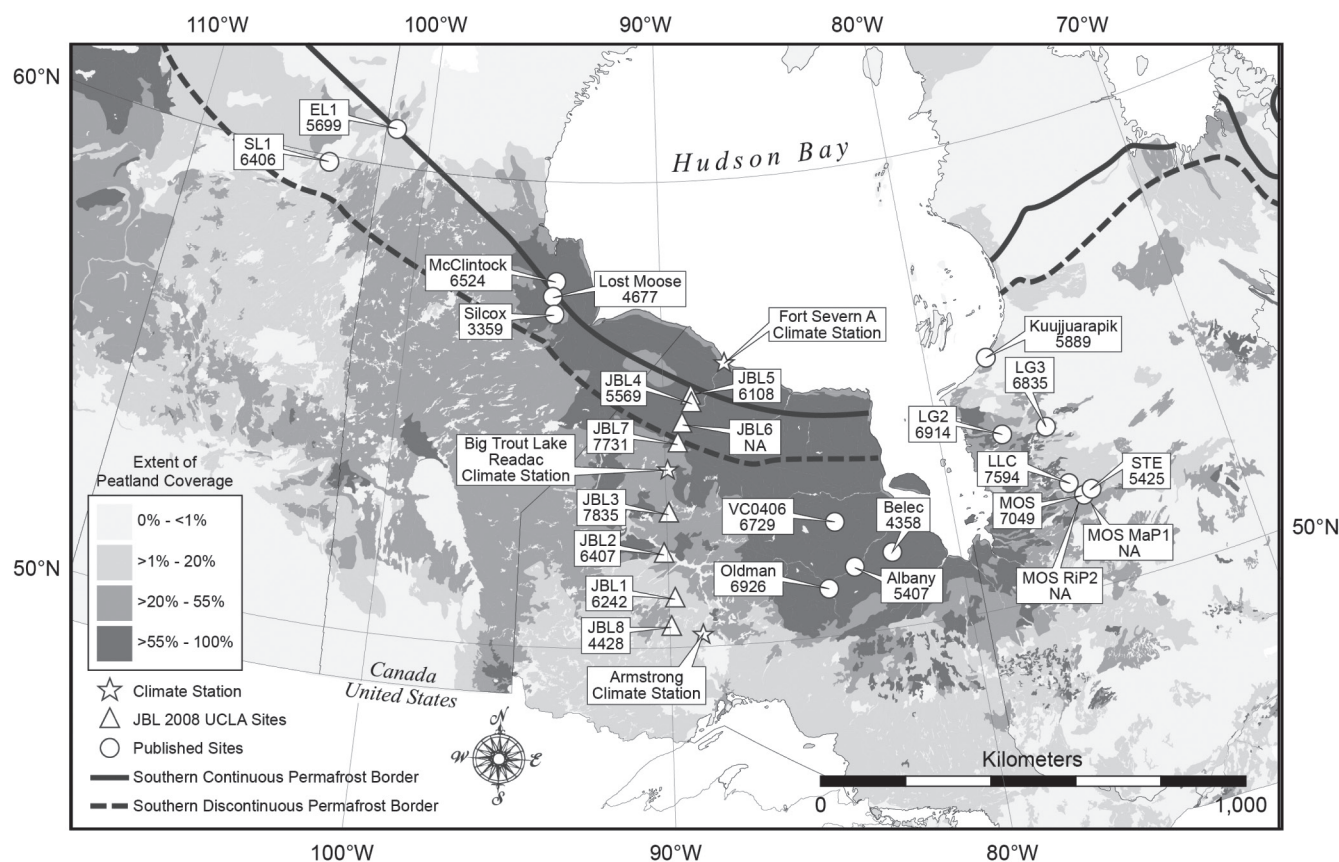


FIGURE 1. Our study sites were located in the James Bay Lowland (JBL), and were supplemented by a review of 17 additional age-depth models from surrounding regions in Canada. Pictured are also maps of peatland extent (Tarnocai et al., 2011), and the borders of discontinuous and continuous permafrost zones (Brown et al., 2001).

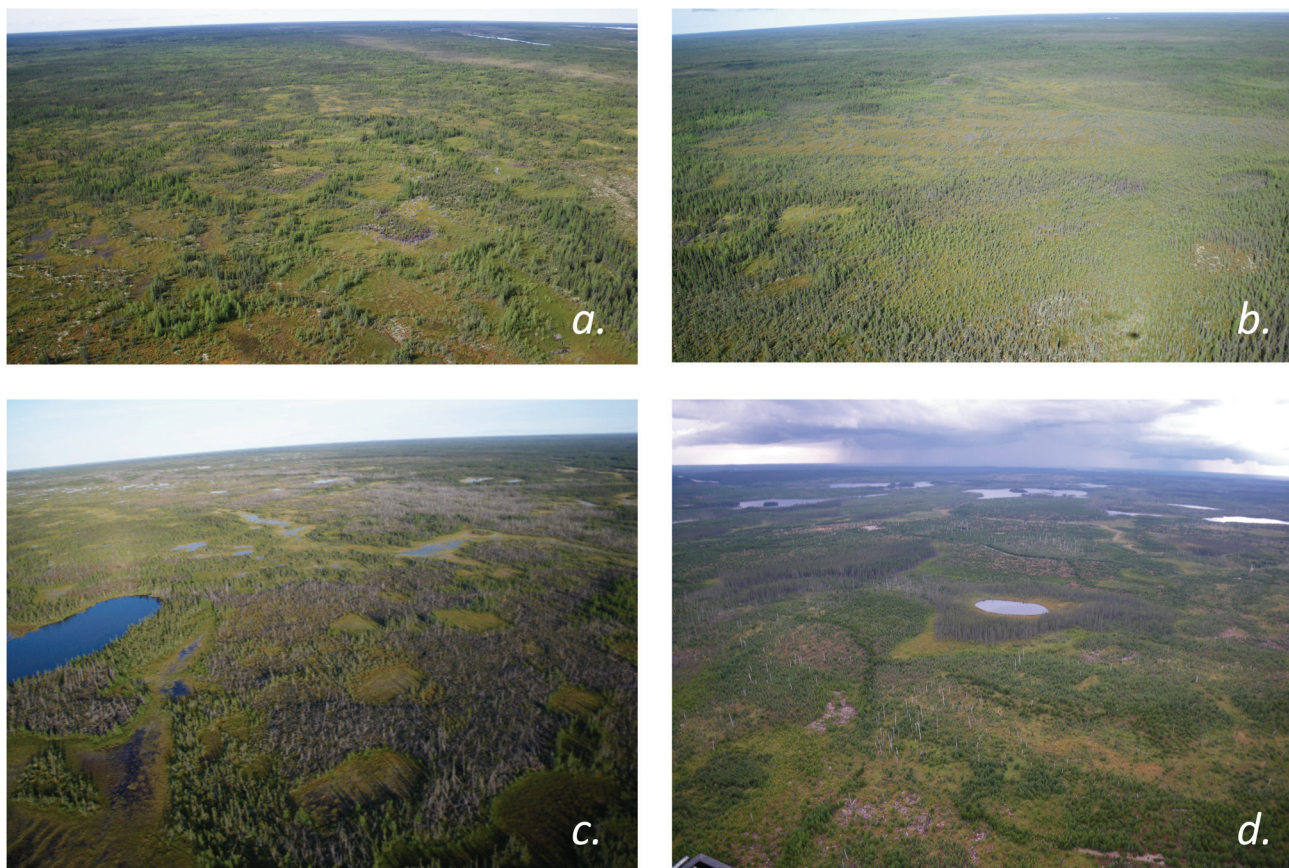


FIGURE 2. Landscapes that are representative of the surface cover in the JBL, including: (a) *Picea mariana* dominated stands, (b) uncovered *Sphagnum* bogs, (c) minerotrophic thin fens, and (d) open water. Photos are courtesy of David Beilman, and are used with permission (Beilman, personal communication).

There were two major objectives of this study. The first was to quantify the initiation time, soil C density, and apparent rate of C accumulation in bog peat in central and northern Ontario for both pre-2 ka and post-2 ka. The second was to determine the effect that climate has had on vertical peat accumulation over the larger area surrounding the Hudson and James Bays. We hypothesized

that apparent C accumulation and 2 ka depth would correlate significantly and inversely with modern mean annual precipitation (MAP), and positively with modern MAAT, GDD_0 , and PAR_0 . We also hypothesized that permafrost occurrence has had a significant effect on peat depth, and 2 ka peatland depth with permafrost would be significantly shallower than non-permafrost locations.

TABLE 1

Site information for 8 new James Bay Lowland and adjacent regions sites collected in the summer of 2008. Sites are listed from south to north.

Core	Latitude, Longitude	Elevation (m)	Peatland type
JBL8	50°27'33"N, 89°55'42"W	407	<i>Sphagnum</i> bog
JBL1	51°03'53"N, 89°47'34"W	371	<i>Sphagnum</i> bog
JBL2	52°01'07"N, 90°07'53"W	362	<i>Sphagnum</i> bog
JBL3	52°51'37"N, 89°55'46"W	270	<i>Sphagnum</i> bog
JBL7	54°23'43"N, 89°31'20"W	150	<i>Sphagnum</i> bog
JBL6	54°46'21"N, 89°19'10"W	140	Permafrost bog
JBL4	55°16'09"N, 88°55'50"W	108	<i>Sphagnum</i> bog
JBL5	55°24'55"N, 88°57'06"W	143	Permafrost plateau

Materials and Methods

FIELD SITES

The Ontario James Bay Lowland (JBL), in which most of the study sites are located (Fig. 1), covers 221,000 km²; 36% of the wetlands present are bogs dominated primarily by *Sphagnum* (Riley, 2005). The Hudson Plains contain *Picea mariana*-dominated forests in the south (Fig. 2) and mixed *P. mariana* and *Larix laricina* forests in the north (Riley, 2005, 2011). These are interspersed with unforested bog and fen complexes dominated by *Sphagnum* mosses and *Carex* sp., respectively (Fig. 2). Northern permafrost bogs have drier surfaces and are often typified by a surface cover of *Cladonia*. The Hudson Plains formed after the last glacial maximum following the retreat of the Laurentide ice sheet commencing at approximately 10 ka. The Hudson Plains remained largely covered with the remaining ice sheet and glacial lakes Agassiz and Ojibway until the first land emergence around 9 ka (Dyke et al., 2003). Many peatlands in the southern lowlands were formed after the catastrophic drainage of the glacial lakes due to the breaking of the Laurentide ice dam around 8.4 ka (Lajeunesse and St-Onge, 2008). The rest of the land gradually became available for peatlands due to isostatic rebound. The Hudson Plains have had some of the fastest rates of isostatic uplift on earth, with some areas rising an average of 1.2 m century⁻¹ (Webber et al., 1970).

Permafrost occurs in the Hudson Bay coast as well as northern regions of the Hudson Bay and James Bay Lowlands. It dominates the landscape in the north within ~80 km of the coast, and occurs along the coast in the south within a slimming margin approximately 20 to 40 km wide (Fig. 1; Riley, 2005). Along the coast, continuous permafrost and subarctic vegetation can be found anywhere where soil temperatures remain below 0 °C annually, and discontinuously south of this isotherm due to the efficient insulating qualities of peat soils (Riley, 2005).

The peatlands of central and northern Ontario are accessible almost exclusively by helicopter, boat, or winter ice road, and remain both sparsely populated and understudied. Some peatland basal dates and paleoecological information are available from studies focused near the Albany River (Glaser et al., 2004), Churchill Rail Line (Dredge and Mott, 2003), and Victor Mine (O'Reilly, 2011; Bunbury et al., 2012). We collected eight bog cores from eight sites by helicopter during the summer of 2008 (Fig. 1; Table 1). The sites form a latitudinal transect between 50°27'N and 55°24'N (Fig. 1; Table 1). All cores were collected from raised, ombrotrophic peat landforms (Table 1). MAP and MAAT data from three climate stations within the approximate range of the sites

are included in Table 2 (Fig. 1; Environment Canada, 2013). In 2008 these climate stations were within the peatlands' temperature-precipitation space described in Yu et al. (2009), ranging from -4.88 to 3.03 °C, and 607.8 to 683.5 mm (Table 2; Environment Canada, 2013).

Six cores—JBL1, JBL2, JBL3, JBL4, JBL7, JBL8—were from *Sphagnum fuscum*-dominated hummock surfaces and were permafrost free (Table 1). These hummocks existed in complexes with *S. angustifolium* hollows and intermediate *S. magellanicum* sections. Hummock-hollow patterning reflects *Sphagnum* species optimal growth and community ecology (Gunnarsson, 2005). Notable vascular species include tree species (*Picea mariana*, *Larix laricina*), shrub species (*Chamaedaphne* sp., *Vaccinium* sp., *Salix* sp., *Betula* sp., *Eriophorum* sp.), as well as *Carex* sp. and *Equisetum* sp. in hollows. JBL2 and JBL3 existed as bog islands in larger poor-fen complexes. JBL4 was from the discontinuous permafrost zone and contained examples of boreal vegetation as well as subarctic *Cladonia* sp. on higher microsites. Two cores, JBL5 and JBL6, were from *Cladonia*-dominated surfaces underlain by *Sphagnum*-dominated permafrost peat (Table 1). JBL5 was a degraded permafrost plateau with large cracks filled with meltwater. JBL5's surface cover was predominantly *Cladonia* sp., *Ledum* sp., and unvegetated surfaces of decayed peat.

At each core site, the first 0.8 to 1 m was sampled with a box corer and the remainder with a Russian auger in non-permafrost peatlands and a motorized SIPRE drill in permafrost. Seven of the cores contained complete profiles from the surface to the mineral/peat interface. JBL6 was recovered without the basal section and is therefore omitted from the pre-2 ka C accumulation and total C accumulation data sets. Cores were wrapped in plastic wrap and aluminum foil and placed in a freezer on arrival at the University of California, Los Angeles. All cores were subsampled, while frozen, in 1 cm increments using a bandsaw.

We supplemented our 8 cores with a review of 17 other cores from a broader geographical region encompassing the Boreal Shield, Hudson Plains region, and Taiga Shield surrounding the Hudson and James Bays. The entire data set ranges in latitude from 50°27'N to 60°50'N (Fig. 1; Tables 1 and 3). MAP for the entire network ranged from 238.0 to 861.50 mm, and MAAT ranged from -8.72 to 0.35 °C from 1975 to 2005 (Matsuura and Willmott, 2009). Out of the combined data set, 19 of the sites are from ombrotrophic bogs, whereas 6 are from permafrost plateaus or polygonal peat formations (Tables 1 and 3). We avoided analyzing cores from fens or sites with chronologies that were less than approximately millennially resolved.

TABLE 2

Climate data for 2008 from 3 stations in the JBL and adjacent regions.

Climate station	Latitude, Longitude	Total precipitation (mm/yr)	MAAT (°C)
Fort Severn A	56°01'12"N, 87°40'48"W	NA	-4.88
Big Trout Lake Readac	53°49'12"N, 89°54'00"W	683.5	-3.13
Armstrong	50°17'24"N, 88°54'36"W	608.7	3.03

MAAT = mean annual air temperature.

TABLE 3
Site information from 17 Hudson Bay Lowlands–JBL and adjacent regions ombrotrophic peat profiles with
millennially resolved age-depth models, listed by author.

Author	Core name	Latitude, Longitude	Elevation (m)	Peatland type
Arlen-Pouliot and Bhiry (2005)	Kuujuarapik	55°20'N, 77°40'W	85	Palsa
Beulieu-Audrey (2009)	LG2	53°39'N, 77°44'W	173	<i>Sphagnum</i> bog
	LG3	53°34'N, 76°08'W	215	<i>Sphagnum</i> bog
Bunbury et al. (2012)	VC0406	52°42'36"N, 84°10'48"W	105	<i>Sphagnum</i> bog
Dredge and Mott (2003)	Lost Moose	57°33.9'N, 94°19.0'W	109	<i>Sphagnum</i> bog
	Silcox	57°10.0'N, 94°14.2'W	141	<i>Sphagnum</i> bog
Glaser et al. (2004)	Albany	51°26'N, 83°37'W	82	<i>Sphagnum</i> bog
	Belec	51°37'N, 82°17'W	64	<i>Sphagnum</i> bog
	Oldman	51°01'N, 84°34'W	101	<i>Sphagnum</i> bog
Kuhry (2008)	McClintock	57°50'N, 94°12'W	80	Permafrost plateau
Sannel and Kuhry (2009)	EL1	60°50'N, 101°33'W	329	Permafrost plateau
	SL1	59°53'N, 104°12'W	390	Permafrost plateau
Loisel and Garneau (2010)	MOS MaP1	51°58'N, 75°24'W	304	<i>Sphagnum</i> bog
	MOS RiP2	51°58'N, 75°24'W	304	<i>Sphagnum</i> bog
van Bellen et al. (2011)	LLC	52°17'15"N, 75°50'21"W	256	<i>Sphagnum</i> bog
	MOS	51°58'55"N, 75°24'06"W	299	<i>Sphagnum</i> bog
	STE	52°02'37"N, 75°10'23"W	303	<i>Sphagnum</i> bog

SOIL C ESTIMATES

We estimated percentage C for every 1 cm increment as the product of dry bulk density (BD), loss on ignition at 550 °C (LOI_{550}), and a %C assumption of 0.5 g C 1 g OM⁻¹ (Turunen et al., 2002). Samples for BD and LOI_{550} were taken from subsampled cores with a stainless steel tube with a 1 cm diameter. Samples were measured lengthwise with digital calipers to calculate volume. Dry BD was measured by dividing the dry weight by the sample volume after drying to a constant mass at 105 °C. LOI_{550} was calculated as the mass lost after one hour ignition in a muffle furnace at 550 °C (Sheng et al., 2004).

AGE DEPTH MODELING

Chronologies for the eight new cores were established using multiple ¹⁴C dates (Table 4). Dates were selected in order to have approximately millennially resolved chronologies before 1 ka, and bicentennially resolved chronologies since 1 ka. Plant macrofossils were separated from peat with distilled H₂O. Fungal hyphae and plant rootlets were removed using forceps under a dissecting microscope. Macrofossils were identified down to the genus level when possible using a

stereomicroscope and Canadian macrofossil identification guides (Lévesque et al., 1988). Bulk peat was used when no single macrofossils were identified. Samples were pre-treated using acid-base-acid treatments at 65 °C to remove carbonates, humic acids, and dissolved organic C (Olsson, 1986). Samples were vacuum-sealed in quartz tubes with CuO powder and Ag wire and combusted for 4 h at 900 °C. Samples were graphitized, and atomized in an accelerator mass spectrometer at the Keck Laboratory at the University of California, Irvine. The ratio of ¹⁴C to ¹²C was calculated relative to blank and standards from dendrochronologically dated wood.

Multiple ¹⁴C dates (Table 4; Appendix Table A1) were calibrated, and an age-depth model was created for each core using ‘Bacon’ (Fig. 3 and Appendix Fig. A1), a flexible Bayesian age-depth modeling software (Blaauw and Christen, 2011) that is coded using the computer language R (R Development Core Team, 2012). Dates were calibrated using INTCAL09 (Reimer et al., 2009), and NH1 for post-bomb dates (Hua and Barbetti, 2007). We assumed a date of –58 BP for the surface of each new core except for JBL5, which had surface peat that dated pre-modern (15 ¹⁴C age; Table 4). Seventeen age-depth models from the previously published sites were recalculated using ‘Bacon’ to standardize methods. The surface date was used as a calibration point if it was listed in the literature.

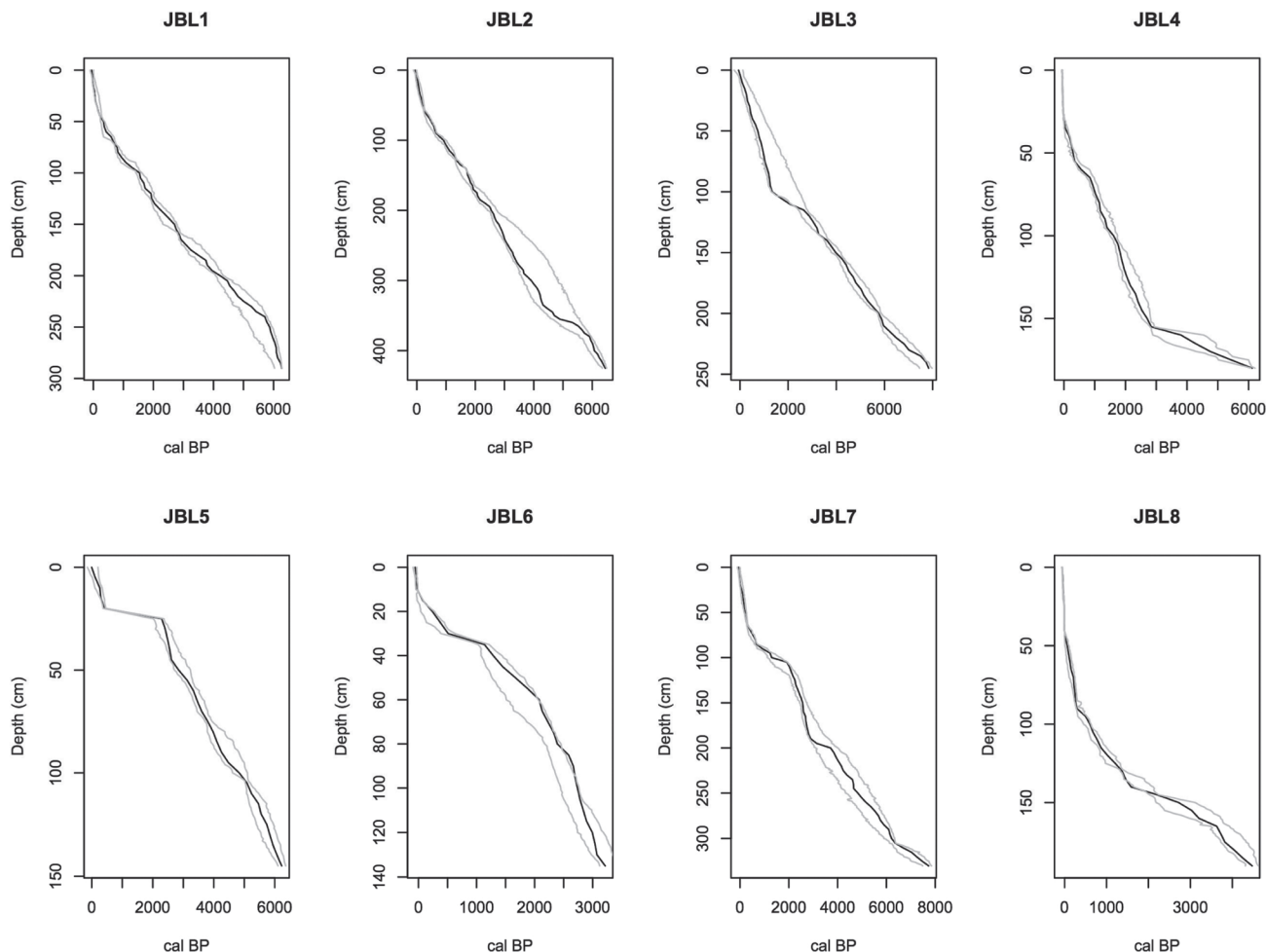


FIGURE 3. ‘Bacon’ age-depth models for 8 new JBL cores. The best estimates for calibrated age are shown in black. The upper and lower estimates are shown in gray.

We preferred ‘Bacon’ to linear interpolation between dates because the latter can be too restrictive if cores are longer than 1 m and do not have high-resolution dating (Blaauw and Heegaard, 2012). ‘Bacon’ deals with outliers in a standardized way using a robust Student’s *t* method (Christen and Pérez, 2011). Bayesian algorithms require priors. We used the program’s default settings for the priors: shape (2), memory strength (4), and memory mean (0.7). For the accumulation rate prior we used a default value of 20 yr cm⁻¹, and used 50 yr cm⁻¹ if the default did not produce a parsimonious age-depth model. Only JBL7 required a different accumulation prior of 40 yr cm⁻¹.

AVERAGE APPARENT RATE OF C ACCUMULATION

We calculated the mass of C accumulated from initiation to the surface, 2 ka depth to the surface, and initiation to 2 ka (Beilman et al., 2009). For average Holocene apparent rate of C accumulation, we summarized the mass of C and divided the mass by the amount of time since initiation. For post-2 ka apparent rate of C accumulation, we summarized the amount of C accumulated since the closest approximation to 2 ka and divided the mass by that closest approximation. For pre-2 ka apparent rate of C accumulation, we

summarized the mass of C accumulated from initiation to 2 ka and divided it by the difference between initiation date and the closest 2 ka date.

STATISTICAL ANALYSIS

We statistically tested hypotheses regarding the relationships between climate and 2 ka depths, as well as permafrost occurrence on both total depths, and 2 ka depths. To test the hypotheses that MAP, MAAT, GDD₀, and PAR₀ correlate significantly with 2 ka depth, we used linear regressions, and climate data from 0.5 × 0.5° integrated gridded databases for MAP and MAAT (1975–2005; Matsuura and Willmott, 2009). Initial analysis and previous research (Beilman et al., 2009) indicated the possibility of an exponential relationship between MAAT and 2 ka depth, so we included an exponential regression in our analysis of these two variables. For measurements involving seasonality we used 0 °C as a base temperature because *Sphagnum* species are adapted to growth at low temperatures (Asada et al., 2003). We calculated a 0.5 × 0.5° gridded database for GDD₀ from daily temperature values and PAR₀ from latitude, orbital parameters, and the fraction of sunshine hours (Prentice

TABLE 4
¹⁴C-AMS samples, depth, ¹⁴C ages, and best fit “Bacon” model calibration estimates for 8 new southwest JBL cores.

Core	Depth (cm)	Lab I.D. #	Material	¹⁴ C age (cal yr B.P.)	±	Age range (cal yr B.P.)	Best fit (cal yr B.P.)	
JBL1	44–45	UCI AMS 107067	<i>Sphagnum</i> stems	110	20	219–274	228	
JBL1	57–58	UCI AMS 90508	Cyperaceae leaf	225	30	288–248	402	
JBL1	70–71	UCI AMS 107068	Moss stem	795	20	664–739	694	
JBL1	83–84	UCI AMS 93975	Cyperaceae stems and rhizome	970	30	805–1055	918	
JBL1	96–97	UCI AMS 115836	Cyperaceae leaves	1565	20	1320–1515	1394	
JBL1	123–124	UCI AMS 91703	Cyperaceae fragment	1985	20	1869–2029	1938	
JBL1	155–156	UCI AMS 90509	Wood	2680	15	2690–2875	2782	
JBL1	195–196	UCI AMS 91704	Cyperaceae fragments	3745	20	3916–4251	4006	
JBL1	239–240	UCI AMS 91705	Amblystegiaceae stems	4960	25	4978–5793	5713	
JBL1	285–286	UCI AMS 67693	Bulk peat	5265	15	5982–6262	6242	
JBL1	285–286	UCI AMS 96178	Amblystegiaceae stems	5195	35	5982–6262	6242	
JBL2	55–56	UCI AMS 90510	<i>Sphagnum</i> stems	75	15	229–264	239	
JBL2	71–72	UCI AMS 91706	<i>Sphagnum</i> stems	375	20	355–555	512	
JBL2	87–88	UCI AMS 90511	Cyperaceae leaf	625	15	564–664	641	
JBL2	103–104	UCI AMS 91707	<i>Sphagnum</i> stems	1065	30	863–1043	950	
JBL2	125–126	UCI AMS 76592	Bulk peat	1390	15	1266–1346	1341	
JBL2	162–163	UCI AMS 97814	Cyperaceae leaves	1915	25	1779–1959	1879	
JBL2	200–201	UCI AMS 67694	Bulk peat	2530	20	2473–2753	2562	
JBL2	267–268	UCI AMS 96179	Cyperaceae leaves	3915	20	3263–4408	4408	
JBL2	324–325	UCI AMS 76591	Bulk peat	3285	20	3933–5173	4237	b.
JBL2	335–336	UCI AMS 93976	Amblystegiaceae stems	3845	30	4156–5311	4349	
JBL2	375–376	UCI AMS 91708	Amblystegiaceae stems	5030	50	5437–5897	5771	
JBL2	420–421	UCI AMS 93977	Amblystegiaceae stems, spruce needles, Cyperaceae leaf	5900	180	6247–6462	6395	
JBL2	421–422	UCI AMS 67695	Bulk peat	5560	20	6265–6460	6407	
JBL3	83–84	UCI AMS 90512	<i>Sphagnum</i> fronds	–625	15	1076–2096	1175	a.,b.
JBL3	95–96	UCI AMS 93978	Cyperaceae leaf, ericaceous leaf fragment	1290	20	1212–2347	1275	
JBL3	111–112	UCI AMS 93979	Cyperaceae leaves	2415	20	2272–2722	2294	
JBL3	135–136	UCI AMS 97815	Cyperaceae leaves	3240	20	3319–3579	3334	
JBL3	151–152	UCI AMS 76593	Bulk peat	3760	15	3963–4213	4079	
JBL3	173–174	UCI AMS 97816	<i>Equisetum</i> fragments	2020	80	4514–5104	4795	b.
JBL3	195–196	UCI AMS 91709	Wood fragments	4920	25	5426–5806	5583	
JBL3	211–212	UCI AMS 90513	Needle fragments	4380	70	5915–6475	6066	b.
JBL3	244–245	UCI AMS 93980	<i>Sphagnum</i> fronds	6930	60	7457–7977	7835	
JBL3	244–245	UCI AMS 67696	Bulk peat	7145	45	7457–7977	7835	
JBL4	25–26	UCI AMS 76594	Bulk peat	–2175	15	–31 to –11	–12	a.
JBL4	36–37	UCI AMS 107070	<i>Sphagnum</i> stems	130	20	29–144	95	
JBL4	45–46	UCI AMS 107071	<i>Sphagnum</i> stems	85	20	122–267	253	
JBL4	54–55	UCI AMS 107072	<i>Sphagnum</i> stems	340	20	326–481	346	
JBL4	64–65	UCI AMS 107073	<i>Sphagnum</i> stems	1030	20	740–985	848	
JBL4	75–76	UCI AMS 76595	Bulk peat	1150	15	975–1180	1054	
JBL4	100–101	UCI AMS 76596	Bulk peat	1750	15	1533–1733	1641	
JBL4	150–151	UCI AMS 76597	Bulk peat	2610	15	2589–2824	2731	
JBL4	167–168	UCI AMS 96180	<i>Picea</i> needle	4325	45	3965–4985	4563	
JBL4	175–176	UCI AMS 67697	Bulk peat	5245	20	5251–6021	5569	
JBL4	175–176	UCI AMS 94022	Moss fronds	5450	110	5251–6021	5569	
JBL5	0–1	UCI AMS 90522	<i>Betula</i> leaf	15	15	–146–204	–5	

TABLE 4
Continued.

Core	Depth (cm)	Lab I.D. #	Material	¹⁴ C age (cal yr B.P.)	±	Age range (cal yr B.P.)	Best fit (cal yr B.P.)	
JBL5	7–8	UCI AMS 107074	Lichen fragments	115	20	75–280	204	
JBL5	11–12	UCI AMS 107075	Bulk peat	–140	20	179–364	277	a., b.
JBL5	15–16	UCI AMS 76598	Bulk peat	300	15	308–423	321	
JBL5	19–20	UCI AMS 107076	<i>Sphagnum</i> stems	360	20	374–459	414	
JBL5	25–26	UCI AMS 107077	<i>Sphagnum</i> stems	2200	20	2064–2379	2315	
JBL5	26–37	UCI AMS 96181	<i>Sphagnum</i> stems	2400	25	2398–2738	2513	
JBL5	55–56	UCI AMS 93981	Herbaceous fragment	2965	20	3055–3315	3170	
JBL5	72–73	UCI AMS 67698	Bulk peat	3420	15	3636–3886	3722	
JBL5	100–101	UCI AMS 76599	Bulk peat	4350	15	4733–5108	4885	
JBL5	140–141	UCI AMS 67699	Bulk peat	5320	20	5949–6294	6108	
JBL5	140–141	UCI AMS 93982	Cyperaceae leaves, spruce needle fragments, moss stems	5170	25	5949–6294	6108	
JBL6	10–11	UCI AMS 90514	Coniferous needles	–1020	15	–46 to –11	–23	a.
JBL6	15–16	UCI AMS 107078	Lichen fragments	125	20	–2–103	73	
JBL6	19–20	UCI AMS 107079	Bulk peat	–90	20	36–226	206	a., b.
JBL6	27–28	UCI AMS 107080	Bulk peat	360	20	281–481	430	
JBL6	33–34	UCI AMS 90515	<i>Sphagnum</i> stems	1165	15	806–966	886	
JBL6	75–76	UCI AMS 67700	Bulk peat	2195	20	2055–2355	2331	
JBL6	100–101	UCI AMS 76600	Bulk peat	2440	15	2448–2773	2520	
JBL6	134–135	UCI AMS 67701	Bulk peat	3025	20	3110–3405	3187	
JBL7	51–52	UCI AMS 76601	Bulk peat	125	15	196–266	225	
JBL7	61–62	UCI AMS 93983	<i>Sphagnum</i> stems	190	15	268–303	283	
JBL7	71–72	UCI AMS 93984	<i>Sphagnum</i> stems	375	20	340–505	468	
JBL7	82–83	UCI AMS 93985	<i>Sphagnum</i> stems	645	20	559–669	656	
JBL7	92–93	UCI AMS 93986	<i>Sphagnum</i> stems	1205	30	955–1195	1103	
JBL7	121–122	UCI AMS 97817	<i>Sphagnum</i> stems	2310	15	2027–2387	2198	
JBL7	150–151	UCI AMS 67702	Bulk peat	2505	15	2471–2741	2569	b.
JBL7	177–178	UCI AMS 96182	Cyperaceae leaves and rhizome	2540	25	2692–3267	2755	
JBL7	205–206	UCI AMS 93987	<i>Sphagnum</i> stems	5190	25	3181–4251	3859	
JBL7	300–301	UCI AMS 67703	Bulk peat	5365	15	5994–6339	6241	
JBL7	327–328	UCI AMS 91710	<i>Sphagnum</i> stems	6840	25	7340–7790	7627	
JBL7	327–328	UCI AMS 93988	Bulk peat	6910	30	7340–7790	7627	
JBL7	329–330	UCI AMS 90516	Wood	3860	15	7487–7847	7731	
JBL8	25–26	UCI AMS 76602	Bulk peat	–1215	15	–11 to –6	–8	a.
JBL8	37–38	UCI AMS 90517	<i>Salix</i> leaf	–535	15	–7 to –7	–6	a.
JBL8	77–76	UCI AMS 91711	<i>Sphagnum</i> fronds	115	20	171–266	228	
JBL8	87–88	UCI AMS 90518	<i>Sphagnum</i> stems	210	15	259–374	280	
JBL8	99–100	UCI AMS 90519	<i>Sphagnum</i> stems	565	15	451–631	603	
JBL8	111–112	UCI AMS 91712	Coniferous needle fragments	950	40	713–913	814	
JBL8	125–126	UCI AMS 76603	Bulk peat	1385	15	1074–1334	1241	
JBL8	140–141	UCI AMS 91713	<i>Sphagnum</i> fronds	2075	20	1748–2143	1710	
JBL8	159–160	UCI AMS 94023	Cyperaceae leaves	3380	60	2983–3723	3205	
JBL8	186–187	UCI AMS 96183	Cyperaceae leaves	1840	70	4208–4568	4337	b.
JBL8	188–189	UCI AMS 67704	Bulk peat	4025	15	4319–4594	4428	

a. Refers to dates that contain ¹⁴C from atomic weapons testing.

b. Refers to outliers that were eliminated by “Bacon.”

TABLE 5

Peatland basal depths, basal ages, and 2 ka depths for 17 review and 8 new JBL and adjacent regions cores. Data for loss on ignition at 550 °C (LOI₅₅₀), mean bulk density (BD), and apparent rate of C accumulation; C mass data since inception, post-2 ka, and pre-2 ka are displayed as well.

Core	Depth (cm)	Basal age (cal yr B.P.)	2 ka depth (cm)	Mean LOI ₅₅₀	Mean BD (g cm ⁻³)	Total		Post-2 ka		Pre-2 ka	
						C mass (kg C m ⁻²)	Apparent rate of C accumulation (g C m ⁻² yr ⁻¹)	C mass (kg C m ⁻²)	Apparent rate of C accumulation (g C m ⁻² yr ⁻¹)	C mass (kg C m ⁻²)	Apparent rate of C accumulation (g C m ⁻² yr ⁻¹)
JBL1	286	6249	128	0.94 ± 0.04	0.098 ± 0.031	129.8	20.8	51.3	25.6	78.5	18.1
JBL2	422	6407	173	0.97 ± 0.02	0.079 ± 0.029	171.2	26.7	62.5	31.2	108.7	24.8
JBL3	245	7835	109	0.94 ± 0.11	0.103 ± 0.092	107.1	13.7	36.5	18.4	70.6	12.2
JBL4	176	5569	122	0.96 ± 0.04	0.086 ± 0.033	71.5	12.8	42.3	21.2	29.3	8.2
JBL5	141	6108	24	0.93 ± 0.08	0.135 ± 0.046	82.0	13.4	16.3	8.5	65.7	15.8
JBL6	NA	NA	58	0.98 ± 0.09	0.084 ± 0.037	NA	NA	28.5	14.3	NA	NA
JBL7	330	7731	109	0.94 ± 0.05	0.08 ± 0.026	129.2	16.7	37.8	18.9	91.4	15.9
JBL8	189	4428	143	0.95 ± 0.03	0.087 ± 0.041	77.1	17.4	49.2	23.7	27.8	11.9
Albany	264	5407	106	—	—	—	—	—	—	—	—
Belec	236	4358	63	—	—	—	—	—	—	—	—
EL1	186	5699	8	—	—	—	—	—	—	—	—
Kuujjuarapik	225	5889	31	—	—	—	—	—	—	—	—
LG2	397	6914	72	—	—	—	—	—	—	—	—
LG3	375	6835	54	—	—	—	—	—	—	—	—
LLC	483	7594	123	—	—	—	—	—	—	—	—
Lost Moose	135	4677	73	—	—	—	—	—	—	—	—
McClintock	166	6524	64	—	—	—	—	—	—	—	—
MOS	297	7049	101	—	—	—	—	—	—	—	—
MOS MaP1	NA	NA	92	—	—	—	—	—	—	—	—
MOS RiP2	NA	NA	74	—	—	—	—	—	—	—	—
Oldman	446	6926	156	—	—	—	—	—	—	—	—
Silcox	70	3359	53	—	—	—	—	—	—	—	—
SL1	196	6406	63	—	—	—	—	—	—	—	—
STE	286	5425	108	—	—	—	—	—	—	—	—
VC0406	304	6729	105	—	—	—	—	—	—	—	—

et al., 1993; Hijmans et al., 2005), using the CLIMATE 2.2 database (Kaplan et al., 2003). We also tested the hypothesis that permafrost peatlands are significantly shallower than non-permafrost peatlands, using a one-way ANOVA with permafrost occurrence as the independent variable, and total depth, or 2 ka depth, as the dependent variable. All statistics were calculated in R (R Development Core Team, 2012).

Results

PEAT INITIATION ESTIMATES, DEPTHS, AND CHRONOLOGIES

A full report of ¹⁴C dates in the eight new cores is available in Figure 1 and Table 4. The timing of peat initiation in the eight new sites followed major deglaciation, glacial lake drainage, and land emergence around 8.34 ka (Dyke et al., 2003). Basal dates

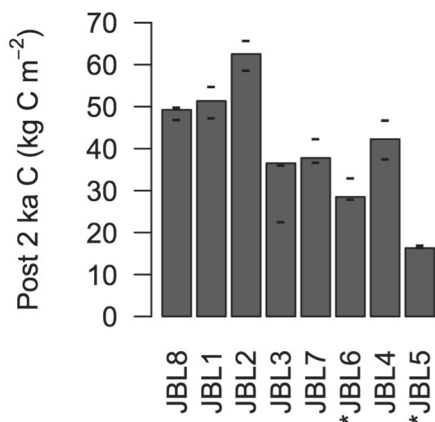


FIGURE 4. Post-2 ka C accumulated in the 8 southwest JBL sites arranged by latitude. (–) Represent the upper and lower estimates of Post-2 ka C masses based on upper and lower estimates of 2 ka by ‘Bacon’ models. (*) Represents permafrost peat.

from the eight new cores vary between 7.8 ka and 4.4 ka, and have an average initiation time of $6.3 \pm (\text{std. dev.}) 1.2$ ka (Fig. 1; Table 5). Peat depth averaged 256 ± 98 cm and ranged from 141 to 422 cm (Table 5). Core lengths from previously published northeastern Canadian studies ranged from 70 to 483 cm, and had a mean of 266 ± 109 cm (Table 5). These mean depths roughly correspond to the average depths estimated for northern peatlands (2.3 m; Gorham, 1991).

SOIL C MASS IN CENTRAL AND NORTHERN ONTARIO

BD in the new cores ranged from 0.0034 to 0.62 g cm^{-3} and averaged $0.093 \pm 0.041 \text{ g cm}^{-3}$ (Table 5). LOI_{550} ranged from 8.7 to 100.0 %OM and averaged 94.5 ± 6.3 %OM. The highest LOI_{550} generally corresponded to the low-density acrotelm and active layer sections. The exception to this is JBL5, which has a densely packed rootlet/lichen active layer (Table 5). The lowest LOI_{550} values generally correspond to highest BD values at the mineral dominated basal sections of JBL3 and JBL5. Our mean organic matter density, 0.087 ± 0.03 is slightly lower than the mean value for fens and bogs in western Canada, 0.094 g cm^{-3} (Vitt et al., 2000a), and the range of measurements from the Mackenzie River Basin, Finland, and the WSL ($0.092\text{--}0.094 \text{ g cm}^{-3}$; Makila, 1994; Sheng et al., 2004; Beilman et al., 2009). There were generally lower BD and higher LOI_{550} in the top meter of peat, and higher BD and lower LOI_{550} in deeper peat due to decay and compaction over time in deeper peat.

More C was older than 2 ka than was younger in the eight new cores. This is not surprising as the pre-2 ka portion of the cores typically represents >5 ka to 2.4 ka of deposition. Pre-2 ka stocks range from 28.3 to $108.7 \text{ kg C m}^{-2}$ and averaged $67.5 \pm 30.0 \text{ kg C m}^{-2}$. Post-2 ka C stocks range from 16.3 to 62.5 kg C m^{-2} and averaged $40.5 \pm 14.3 \text{ kg C m}^{-2}$ (Fig. 4 and Table 5). In central and northern Ontario, about 40% of the total C present in the cores is younger than 2 ka. Notable exceptions to this trend were JBL4 and JBL8 where pre-2 ka apparent rate of C accumulation was drastically lower than post-2 ka (Table 5).

Apparent rate of C accumulation was generally higher post-2 ka than total in the eight new cores. Average apparent rate of C accumulation since initiation ranged from 12.8 to 26.7

$\text{g C m}^{-2} \text{ yr}^{-1}$, with a mean of $17.4 \pm 5.0 \text{ g C m}^{-2} \text{ yr}^{-1}$ (Table 5). These values correspond to estimates of 13 to $30 \text{ g C m}^{-2} \text{ yr}^{-1}$ for North American peat bogs (Gorham, 1991; Turunen et al., 2002; Kuhry and Turunen, 2006), and fall in the range of observed global peatland C accumulation (8.4 to $38.0 \text{ g C m}^{-2} \text{ yr}^{-1}$; Yu et al. 2009). Post-2 ka apparent rate of C accumulation ranged from 8.5 to $30.8 \text{ g C m}^{-2} \text{ yr}^{-1}$ and had an average of $20.2 \pm 6.9 \text{ g C m}^{-2} \text{ yr}^{-1}$. The lowest post-2 ka estimate in JBL5 ($8.5 \text{ g C m}^{-2} \text{ yr}^{-1}$) roughly corresponds with projected rates for subarctic Canada ($9 \text{ g C m}^{-2} \text{ yr}^{-1}$; Gorham, 1991), and the lowest observed arctic estimates from a global synthesis ($8.4 \text{ g C m}^{-2} \text{ yr}^{-1}$; Yu et al. 2009). Pre-2 ka apparent rate of C accumulation was generally lower than post-2 ka apparent rate of C accumulation and ranged from 8.2 to $24.8 \text{ g C m}^{-2} \text{ yr}^{-1}$ and averaged $15.0 \pm 5.6 \text{ g C m}^{-2} \text{ yr}^{-1}$ (Table 5).

In the eight new sites, both apparent rate of C accumulation and 2 ka depth correlate significantly and positively with MAP with r^2 values of 0.56 and 0.58, respectively ($p < 0.05$; Table 6). 2 ka depths also correlate significantly and positively with MAAT ($p < 0.05$; $r^2 = 0.52$; Table 6).

CLIMATE AND 2 KA DEPTH

Based on the combined data set of our 8 new cores and the 17 previously published cores, peat depth at 2 ka correlated significantly and positively with MAP, MAAT, GDD_0 , and PAR_0 . Depths at 2 ka ranged from 8 to 173 cm with a mean of 88.5 ± 41.1 cm (Table 5). Overall peat depth ranged from 70 to 483 cm, meaning that the average proportion of peat vertical accumulation since 2 ka was $36.9 \pm 19.1\%$, roughly similar to the 40% of C present that was younger than 2 ka in our eight new sites. Depth at 2 ka correlates significantly and positively with MAP ($p < 0.05$; $r^2 = 0.20$; Fig. 5; Table 6), MAAT ($p < 0.001$; $r^2 = 0.46$; Fig. 5; Table 6), GDD_0 ($p < 0.0001$; $r^2 = 0.60$; Fig. 5; Table 6), and PAR_0 ($p < 0.0001$; $r^2 = 0.62$; Fig. 5; Table 6). An exponential regression between MAAT and 2 ka depth increased the r^2 value to 0.49 ($p < 0.0001$; Fig. 5; Table 6). A linear regression defining PAR_0 as a predictor of 2 ka depth describes the most variance out of all of the variables we tested (Fig. 5; Table 6).

PERMAFROST OCCURRENCE AND PEAT DEPTH

Permafrost occurrence was found to have a significant effect on 2 ka depths, and on total depths in the 25 new and review cores. A one-way ANOVA determined that there was a statistically significant difference between the depths of permafrost peatlands, and non-permafrost peatlands ($p < 0.05$). A one-way ANOVA showed that permafrost peatlands have a significantly shallower 2 ka depth than non-permafrost peatlands ($p < 0.0001$; Fig. 6). Permafrost total depths averaged 182.8 ± 31.6 cm, whereas non-permafrost total depth averages 290.6 ± 112.0 cm. Permafrost 2 ka depths averaged 41.3 ± 23.6 cm for permafrost peatlands, while non-permafrost bogs averaged 103.4 ± 33.4 cm (Fig. 6).

Discussion

PEATLAND INITIATION

Peatland initiation followed major deglaciation in central and northern Ontario. The oldest site (JBL3) occurred in an area that deglaciation models indicate was at, or near, major glacial

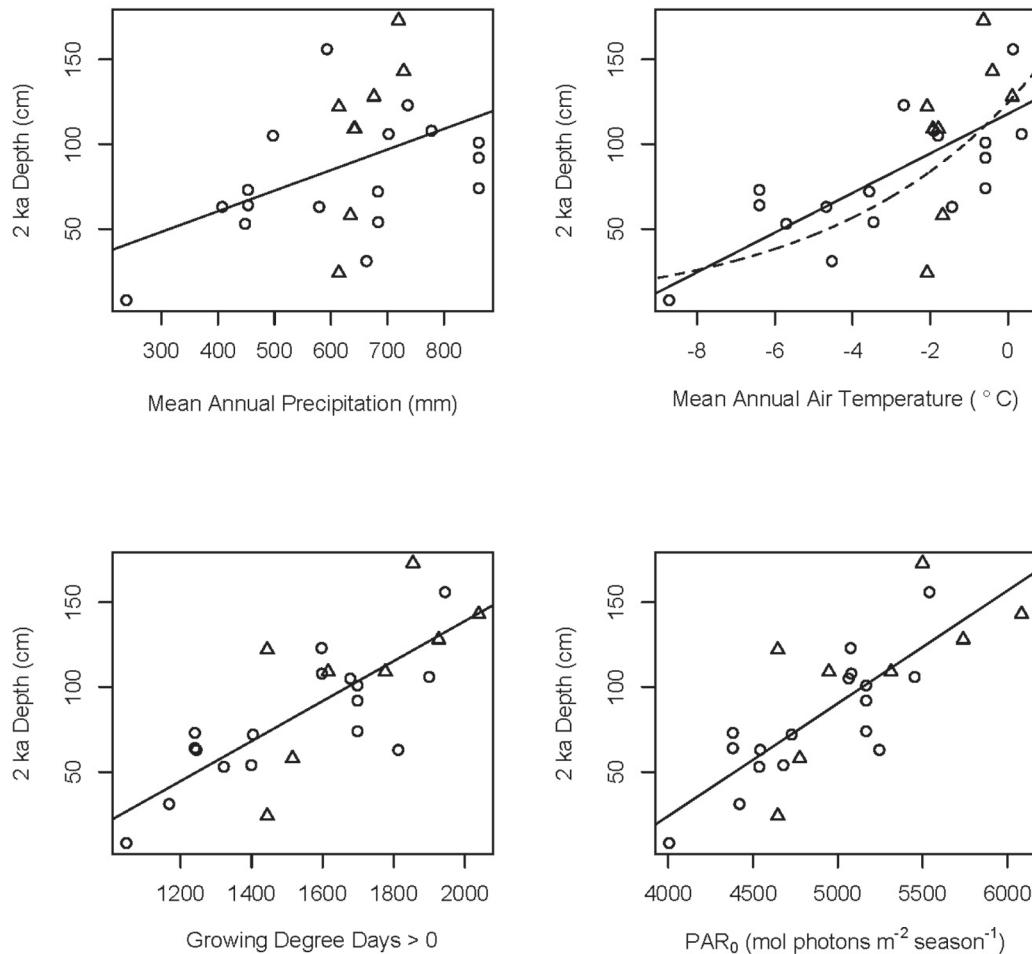


FIGURE 5. Four scatterplots correlating 2 ka depth as a function of environmental variables. Figures are arranged from left to right and top to bottom in order of the linear model's r^2 value. Solid lines represent the best fit for linear regressions. Dashed lines represent the best fit for an exponential regression. Triangles represent new JBL site data. Circles represent review data.

TABLE 6

Correlation statistics for James Bay Lowland (JBL) peatland 2 ka apparent rate of C accumulation, 2 ka depths, and Hudson Bay Lowlands (HBL)–JBL synthesis with mean annual precipitation (MAP), mean annual air temperature (MAAT), growing degree days above 0 °C (GDD_0), and photosynthetically active radiation integrated over the growing season (PAR_0).

	New sites Post-2 ka apparent C accumulation rate ($n = 8$)	New sites 2 ka depth ($n = 8$)	HBL–JBL synthesis 2 ka depth ($n = 25$)
MAP	0.56*	0.58*	0.20*
MAAT	0.38	0.52*	0.46**/0.49*** ^e
GDD_0	0.50	0.50	0.60***
PAR_0	0.46	0.46	0.62***

*Refers to significance at $p < 0.05$.

**Refers to significance at $p < 0.001$.

***Refers to significance at $p < 0.0001$.

^e Refers to an exponential regression rather than a linear regression.

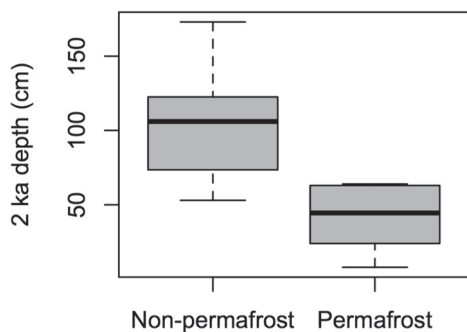


FIGURE 6. Bar and whisker plot of 2 ka depths in permafrost and non-permafrost peat. Central lines represent medians. Box edges represent the 25% upper and lower quantiles. Whisker lines represent least and greatest values.

lake drainage (Dyke et al., 2003). Basal dates show a lag between land availability and peat initiation in North America (Hasley et al., 2000; Gorham et al., 2007), and this is likely the case in eastern Canada. Previous studies describe an average 4000-year lag between deglaciation and widespread peat development due to the time it takes for land to become amenable to peat formation, and due to the random chance of dispersal and colonization of peat-forming species (Hasley et al., 2000). The drainage of post-glacial lakes around 8.34 ka is a likely lag factor (Hasley et al., 2000). Another factor may be a delayed Holocene Thermal Maximum in the North Atlantic caused by cooling from the remainder of the decaying Laurentide ice sheet as late as 6 ka (Kaplan and Wolfe, 2006).

There was a high rate of peat initiation between 6 and 7.8 ka in central and northern Ontario (Fig. 1). However, the eight new initiation estimates do not show a clear stratification with newer initiation occurring closest to the James Bay coast. The youngest core (JBL8) occurs at the southernmost end of the transect, whereas the oldest (JBL3) occurs in the middle (Fig. 1). Stratification of initiation was discussed by a study closer to the southwest coast of the JBL near the Albany River, where rates of isostatic uplift are the highest (Fig. 1; Glaser et al., 2004). This difference is likely due to the fact that catastrophic drainage of glacial lakes Agassiz and Ojibway were responsible for land emergence in some of the eight new sites, rather than gradual isostatic uplift that drives initiation in the Albany River region (Glaser et al., 2004).

C ACCUMULATION IN CENTRAL AND NORTHERN ONTARIO

C accumulation measurements in the eight new sites showed that 40% of C was younger than 2 ka in *Sphagnum* bogs. This is roughly comparable to estimates for WSL, where 41% of C is younger than 2 ka (Sheng et al., 2004; Beilman et al., 2009). Only two of our sites, JBL4 and JBL8, have more post-2 ka C than pre-2 ka C, which may have been caused by low relative pre-2 ka accumulation, relatively high belowground C mineralization, or a combination of both. Apparent rate of C accumulation is the result of autogenic drivers, allogenic drivers, and complex internal ecohydrological feedbacks, and has the potential to vary substantially among peatlands (Belyea and Baird, 2006).

MAAT, GDD₀, AND PAR₀ AS DRIVERS OF POST-2 KA VERTICAL PEAT ACCUMULATION

In our analysis, differing scales showed different correlations between post-2 ka apparent rate of C accumulation, 2 ka depth, and four climate variables. In the eight new sites, MAP correlated significantly with both post-2 ka apparent rate of C accumulation and 2 ka depth. This correlation was also significant and positive in our review data set, but was low relative to MAAT, GDD₀, and PAR₀. MAP may exercise some local control over peat accumulation in the Boreal Shield and Hudson Plains of Ontario, but temperature, seasonality, and photosynthetically active radiation are likely the major drivers of vertical peat accumulation in all peatlands bordering the Hudson and James Bays. This supports the conclusions of a recent global synthesis of peatland C accumulation rates. Water table depths need to be persistently high for peat to form; however, if they are present, they do not explain any of the variance of C accumulation rates (Charman et al., 2013). It is also possible that small sample size in the new sites ($n = 8$) may lower the data set's descriptive power.

In the overall synthesis, there was a significant and positive correlation between 2 ka and MAP ($p < 0.05$; Table 6); however, we did not observe the inverse relationship with precipitation similar to that reported by a broad survey of North American peatlands (Gorham et al., 2003). This may be due to the topographic controls in southern sites (Gorham et al., 2003) that are not present in the more topographically homogeneous Hudson Plains, which we heavily sampled. This was also not a robust relationship because the correlation was heavily influenced by EL1 site data (MAP = 208 mm, 2 ka depth = 8 cm). If that point is deleted, the r^2 value lowers to 0.087, and the statistical significance is eliminated.

Our study showed that MAAT had a significant effect on vertical peat accumulation since 2 ka in northeastern Canada (Fig. 5; Table 6). This is analogous to the relationship found between MAAT and 2 ka depth in WSL; however, there are key differences between the two areas. In WSL, data fits an exponential regression that explains more variation ($r^2 = 0.82$; Beilman et al., 2009) than does our data's exponential regression ($r^2 = 0.49$; Table 6). In WSL there was less variability in 2 ka depth for permafrost sites, as well as deeper 2 ka depths in southern non-permafrost bogs (Beilman et al., 2009).

Our hypotheses, that GDD₀ and PAR₀ are major drivers of peat accumulation, were supported by significant and positive correlations between these variables and 2 ka depths. PAR₀ had the highest correlation ($p < 0.0001$, $r^2 = 0.62$; Table 6). In a previous study that analyzed global *Sphagnum* productivity, a linear regression between PAR₀ and *Sphagnum* productivity explained a significant but comparatively small amount of variance ($r^2 = 0.23$; Loisel et al., 2012). PAR₀ integrates photosynthetically active radiation over the growing season length and can potentially influence two different aspects of peat formation. Photosynthetically active radiation and growing season length may both drive plant growth, and thus litter input (Clymo et al., 1998). Growing season length also affects the length of time each year that the ground is unfrozen and biomass can pass from the acrotelm to the catotelm (Clymo et al., 1998; Gorham et al., 2003). Our results also support a global study of peatland apparent rate of C accumulation over the last 1000 years, in which GDD₀ and PAR₀ were found to correlate significantly with post-1 ka apparent rate of C accumulation (Charman et al., 2013). However, the significance of radiation as a driver of *Sphagnum* growth has been debated because of the high degree of shading in boreal peat bogs, and because of photoinhibition in *Sphagnum* photosynthetic tissues (Harley et al., 1989; Murray et al., 1993).

The relationship of growing season length and photosynthetically active radiation on vertical peat accumulation is important because northern latitudes will be disproportionately affected by global warming. Models of future anthropogenic climate forcing predict disproportionate seasonality changes in northern latitudes, and increases in the length of the growing season (Pachauri and Reisinger, 2007). Between 1982 and 1999 the effective start of the growing season advanced 5.4 days in the northern hemisphere (Jeong et al., 2011). Remote sensing images indicate that the plant growth in the Canadian Low Arctic has increased 0.46–0.67% yr⁻¹ from 1982 to 2006 (Jia et al., 2009). However, there will likely be complications modeling PAR₀ as a predictive bioclimatic variable because of the uncertainty in model prediction of future cloud cover (Charman et al., 2013).

THE EFFECT OF PERMAFROST ON PEAT DEPTH

Significantly shallower basal depths and 2 ka depths in permafrost peatlands compared to peatlands that were permafrost-free supported our hypothesis that permafrost occurrence inhibits peat accumulation and that permafrost occurrence significantly decreased post-2 ka vertical accumulation. This was supported by significantly shallower 2 ka depths in permafrost peat, compared to non-permafrost peat ($p < 0.0001$). Previous studies indicated that permafrost likely formed in western Canada during the Little Ice Age (Vitt et al., 2000b) during the late Holocene. However, the timing of permafrost formation in eastern Canada is not as well understood. Overall shallower permafrost peat may be explained either by permafrost establishment earlier than 2 ka, or by general lower productivity due to constantly lower MAAT, GDD₀, and PAR₀ without the direct influence of permafrost.

There was consistent vertical growth in peatlands post-2 ka. Only two cores, JBL5 and EL1, contained near-surface macrofossils that dated pre-modern. JBL5 had dates of 204 and 207 yr BP at 8 and 12 cm, respectively (Table 4), and EL1 had a 13 cm depth dating near 3.0 ka (Appendix Table A1). Besides these two sites, there is little evidence for the recent shutdown by permafrost of 2 ka C accumulation described in the WSL (Beilman et al., 2009). This study showed reduced but ongoing vertical accumulation, similar to the described activity in a survey of subarctic palsas (Olefelt et al., 2012).

Controls by permafrost of late Holocene peat growth show that productivity, rather than decay, currently drives the significant climatically related differences in peat growth observed here. However, the resulting changes in hydrology and CH₄ emissions from melting permafrost will likely result in a greater uncertainty in peatland C cycle feedbacks (Pachauri and Reisinger, 2007). Past studies of northern and southern regions in the Hudson Plains show that CH₄ emissions were lower than previously estimated (Roulet et al., 1994). If non-permafrost peatlands store C faster than permafrost peatlands, then peatlands could act as a negative feedback to future warming (Turetsky et al., 2007; Beilman et al., 2009) or at least as transient reactions to warming. The effect of permafrost melt on hydrology is also controversial. Some studies project that permafrost melts will increase drainage (Jorgenson and Osterkamp, 2005; Riordan et al., 2006), while others claim that it will increase peatland extent (Payette et al., 2004).

Conclusion

At eight new study sites from the Boreal Shield and Hudson Plains of Ontario, peatland initiation was concentrated between 6 ka and 7.8 ka and lagged land emergence following deglaciation, major glacial lake drainage, and isostatic rebound. Following initiation, peatlands have acted as a sink of atmospheric CO₂. Younger initiations are also present (as late as 3.4 ka) in our data set. Of the eight peatlands that we studied, approximately 40% of their total soil C, 16.3 to 62.5 kg C m⁻², is younger than 2 ka. Average rates of apparent C accumulation post-2 ka are 20.2 ± 6.9 g C m⁻² yr⁻¹. Across the Boreal Shield, Hudson Plains, and Taiga Shield surrounding the Hudson and James Bays, vertical peat growth since 2 ka correlates significantly and positively with modern mean annual precipitation. Depth at 2 ka also correlates significantly and positively with atmospheric thermal properties, and most closely with photosynthetically active radiation integrated over the growing season. There is also evidence for significantly reduced, although continuing, post-2 ka peat accumulation in permafrost bogs. These two pieces of evidence suggest the possibility that initial increased productivity of northern peatlands due to projected climate change in the 21st century and the arctic amplification of warming could produce increased C storage and a potential negative feedback to potential climate warming at least in a transient fashion until the climatic envelope for peatland maintenance is exceeded in northern regions.

Acknowledgments

The authors acknowledge the U.S. National Science Foundation for funding this research (NSF-0843685; NSF-0628598). We also acknowledge Dave Beilman for contributions to fieldwork; Matt Zebrowski for mapping assistance; and Siduo Zhang, Luis Rodriguez, Jennifer Kim, Karly Wagner, and Nicolai Kondov for contributions to laboratory processing. We also thank Nigel T. Roulet and one anonymous reviewer for their constructive criticisms and suggestions for improving this manuscript. We finally thank the people of the communities of Thunder Bay, Pickle Lake, and Big Trout Lake for their assistance and hospitality.

References Cited

- Arlen-Pouliot, Y., and Bhiry, N., 2005: Palaeoecology of a palsa and a filled thermokarst pond in a permafrost peatland, subarctic Québec, Canada. *The Holocene*, 15(3): 408–419.
- Asada, T., Warner, B. G., and Banner, A., 2003: Growth of mosses in relation to climate factors in a hypermaritime coastal peatland in British Columbia, Canada. *The Bryologist*, 106(4): 516–527.
- Beaulieu-Audy, V., Garneau, M., Richard, P. J., and Asnong, H., 2009: Holocene palaeoecological reconstruction of three boreal peatlands in the La Grande Riviere region, Quebec, Canada. *The Holocene*, 19(3): 459–476.
- Beilman, D. W., MacDonald, G. M., Smith, L. C., and Reimer, P. J., 2009: Carbon accumulation in peatlands of West Siberia over the last 2000 years. *Global Biogeochemical Cycles*, 23(1): GB1012, doi: <http://dx.doi.org/10.1029/2007GB003112>.
- Belyea, L. R., and Baird, A. J., 2006: Beyond “the limits to peat bog growth”: cross-scale feedback in peatland development. *Ecological Monographs*, 76(3): 299–322.
- Blaauw, M., and Christen, J. A., 2011: Flexible paleoclimate age-depth models using an autoregressive gamma process. *Bayesian Analysis*, 6(3): 457–474.

- Blaauw, M., and Heegaard, E., 2012: Estimation of age-depth relationships. In Birks, H. J. B., Lotter, A. F., Juggins, S., and Smol, J. P. (eds.), *Tracking Environmental Change Using Lake Sediments*. Vol. 5, Data Handling and Numerical Techniques. Dordrecht, Springer, 379–413.
- Blodau, C., 2002: Carbon cycling in peatlands: a review of processes and controls. *Environmental Reviews*, 10(2): 111–134.
- Breeuwer, A., Heijmans, M. M., Robroek, B. J., and Berendse, F., 2008: The effect of temperature on growth and competition between *Sphagnum* species. *Oecologia*, 156(1): 155–167.
- Bridgman, S. D., Megonigal, J. P., Keller, J. K., Bliss, N. B., and Trettin, C., 2006: The carbon balance of North American wetlands. *Wetlands*, 26(4): 889–916.
- Brown, J., Ferrians, O. J., Jr., Heginbottom, J. A., and Melnikov, E. S., 1998 revised February 2001]: Circum-Arctic map of permafrost and ground-ice conditions. Boulder, Colorado: National Snow and Ice Data Center/World Data Center for Glaciology. Digital Media (accessed 13 August 2012).
- Bunbury, J., Finkelstein, S. A., and Bollmann, J., 2012: Holocene hydro-climatic change and effects on carbon accumulation inferred from a peat bog in the Attawapiskat River watershed, Hudson Bay Lowlands, Canada. *Quaternary Research*, 78: 275–284.
- Carlson, M., Chen, J., Elgie, S., Henschel, C., Montenegro, Á., Roulet, N., Scott, N., Tarnocai, C., and Wells, J., 2010: Maintaining the role of Canada's forests and peatlands in climate regulation. *The Forestry Chronicle*, 86(4): 434–443.
- Charman, D. J., Beilman, D. W., Blaauw, M., Booth, R. K., Brewer, S., Chambers, F. M., Christen, J. A., Gallego-Sala, A., Harrison, S. P., Hughes, P. D. M., Jackson, S. T., Korhola, A., Mauquoy, D., Mitchell, F. J. G., Prentice, I. C., van der Linden, M., De Vleeschouwer, F., Yu, Z. C., Alm, J., Bauer, I. E., Corish, Y. M. C., Garneau, M., Hohl, V., Huang, Y., Karofeld, E., Le Roux, G., Loisel, J., Moschen, R., Nichols, J. E., Nieminen, T. M., MacDonald, G. M., Phadtare, N. R., Rausch, N., Sillasoo, Ü., Swindles, G. T., Tuittila, E.-S., Ukonmaanaho, L., Välranta, M., van Bellen, S., van Geel, B., Vitt, D. H., and Zhao, Y., 2013: Climate-related changes in peatland carbon accumulation during the last millennium. *Biogeosciences*, 10: 929–944.
- Christen, J. A., and Pérez, S., 2011: A new robust statistical model for radiocarbon data. *Radiocarbon*, 51(3): 1047–1059.
- Clymo, R. S., 1984: The limits to peat bog growth. *Philosophical Transactions of the Royal Society of London. B, Biological Sciences*, 303(1117): 605–654.
- Clymo, R. S., Turunen, J., and Tolonen, K., 1998: Carbon accumulation in peatland. *Oikos*, 81: 368–388.
- Davidson, E. A., and Janssens, I. A., 2006: Temperature sensitivity of soil carbon decomposition and feedbacks to climate change. *Nature*, 440(7081): 165–173.
- Dise, N. B., 2009: Peatland response to global change. *Science*, 326(5954): 810.
- Dredge, L. A., and Mott, R. J., 2003: Holocene pollen records and peatland development, northeastern Manitoba. *Géographie physique et Quaternaire*, 57(1): 7–19.
- Dunn, C., and Freeman, C., 2011: Peatlands: our greatest source of carbon credits? *Carbon Management*, 2(3): 289–301.
- Dyke, A. S., Moore, A., and Robertson, L., 2003: GEOSCAN Database. Natural Resources Canada, <<http://geoscan.ess.nrcan.gc.ca>> (accessed 5 February 2010).
- Environment Canada, 2013: National Climate Data and Information Archive. Environment Canada, <<http://www.climate.weatheroffice.gc.ca>> (accessed 7 January 2013).
- Eppinga, M. B., de Ruiter, P. C., Wassen, M. J., and Rietkerk, M., 2009: Nutrients and hydrology indicate the driving mechanisms of peatland surface patterning. *The American Naturalist*, 173(6): 803–818.
- Freeman, C., Fenner, N., and Shirsat, A. H., 2012: Peatland geoengineering: an alternative approach to terrestrial carbon sequestration. *Philosophical Transactions of the Royal Society A: Mathematical, Physical and Engineering Sciences*, 370(1974): 4404–4421.
- Frolking, S., and Roulet, N. T., 2007: Holocene radiative forcing impact of northern peatland carbon accumulation and methane emissions. *Global Change Biology*, 13(5): 1079–1088.
- Frolking, S., Roulet, N. T., Tuittila, E., Bubier, J. L., Quillet, A., Talbot, J., and Richard, P. J. H., 2010: A new model of Holocene peatland net primary production, decomposition, water balance, and peat accumulation. *Earth System Dynamics Discussions*, 1: 115–167.
- Glaser, P. H., Hansen, B., Siegel, D. I., Reeve, A. S., and Morin, P. J., 2004: Rates, pathways and drivers for peatland development in the Hudson Bay Lowlands, northern Ontario, Canada. *Journal of Ecology*, 92(6): 1036–1053.
- Gorham, E., 1991: Northern peatlands: role in the carbon cycle and probable responses to climatic warming. *Ecological applications*, 1(2): 182–195.
- Gorham, E., Janssens, J. A., and Glaser, P. H., 2003: Rates of peat accumulation during the postglacial period in 32 sites from Alaska to Newfoundland, with special emphasis on northern Minnesota. *Canadian Journal of Botany*, 81(5): 429–438.
- Gorham, E., Lehman, C., Dyke, A., Janssens, J., and Dyke, L., 2007: Temporal and spatial aspects of peatland initiation following deglaciation in North America. *Quaternary Science Reviews*, 26(3): 300–311.
- Gunnarsson, U., 2005: Global patterns of *Sphagnum* productivity. *Journal of Bryology*, 27(3): 269–279.
- Halsey, L. A., Vitt, D. H., and Gignac, L. D., 2000: *Sphagnum*-dominated peatlands in North America since the last glacial maximum: their occurrence and extent. *The Bryologist*, 103(2): 334–352.
- Harley, P. C., Tenhunen, J. D., Murray, K. J., and Beyers, J., 1989: Irradiance and temperature effects on photosynthesis of tussock tundra *Sphagnum* mosses from the foothills of the Philip Smith Mountains, Alaska. *Oecologia*, 79(2): 251–259.
- Hijmans, R. J., Cameron, S. E., Parra, J. L., Jones, P. G., and Jarvis, A., 2005: Very high resolution interpolated climate surfaces for global land areas. *International Journal of Climatology*, 25(15): 1965–1978.
- Hua, Q., and Barbetti, M., 2007: Review of tropospheric bomb ¹⁴C data for carbon cycle modeling and age calibration purposes. *Radiocarbon*, 46(3): 1273–1298.
- Jeong, S., Ho, C., Gim, H., and Brown, M. E., 2011: Phenology shifts at start vs. end of growing season in temperate vegetation over the northern hemisphere for the period 1982–2008. *Global Change Biology*, 17(7): 2385–2399.
- Jia, G. J., Epstein, H. E., and Walker, D. A., 2009: Vegetation greening in the Canadian Arctic related to decadal warming. *Journal of Environmental Monitoring*, 11(12): 2231–2238.
- Jorgenson, M. T., and Osterkamp, T. E., 2005: Response of boreal ecosystems to varying modes of permafrost degradation. *Canadian Journal of Forest Research*, 35(9): 2100–2111.
- Kaplan, J. O., Bigelow, N. H., Bartlein, P. J., Christensen, T. R., Cramer, W., Harrison, S. P., Matveyeva, N. V., McGuire, A. D., Murray, D. F., Prentice, I. C., Razzhivin, V. Y., Smith, B., Walker, D. A., Anderson, P. M., Andreev, A. A., Brubaker, L. B., Edwards, M. E., Lozhkin, A. V., and Ritchie, J., 2003: Climate change and Arctic ecosystems II: modeling, palaeodata-model comparisons, and future projections. *Journal of Geophysical Research–Atmospheres*, 108: 8171, doi: <http://dx.doi.org/10.1029/2002JD002559>.
- Kaplan, M. R., and Wolfe, A. P., 2006: Spatial and temporal variability of Holocene temperature in the North Atlantic region. *Quaternary Research*, 65(2): 223–231.
- Kaufman, D. S., Schneider, D. P., McKay, N. P., Ammann, C. M., Bradley, R. S., Briffa, K. R., Miller, G. H., Otto-Bliesner, B. L., Overpeck, J. T., Vinther, B. M., Arctic Lakes 2k Project Members: Abbott, M., Axford, Y., Bird, B., Birks, H. J. B., Bjune, A. E., Briner, J., Cook, T., Chipman, M., Francus, P., Gajewski, K., Geirsdóttir, Á., Hu F. S., Kutchko, B.,

- Lamoureux, S., Loso, M., MacDonald, G., Peros, M., Porinchu, D., Schiff, C., Seppä, H., and Thomas, E., 2009: Recent warming reverses long-term Arctic cooling. *Science*, 325(5945): 1236–1239.
- Kuhry, P., 2008: Palsa and peat plateau development in the Hudson Bay Lowlands, Canada: timing, pathways and causes. *Boreas*, 37(2): 316–327.
- Kuhry, P., and Turunen, J., 2006: The postglacial development of boreal and subarctic peatlands. *Boreal and Peatland Ecosystems*, 188: 21–46.
- Laiho, R., 2006: Decomposition in peatlands: reconciling seemingly contrasting results on the impacts of lowered water levels. *Soil Biology and Biochemistry*, 38(8): 2011–2024.
- Lajeunesse, P., and St-Onge, G., 2008: The subglacial origin of the Lake Agassiz–Ojibway final outburst flood. *Nature Geoscience*, 1(3): 184–188.
- Lévesque, P. E. M., Diné, H., and Larouche, A., 1988: *Guide to the Identification of Plant Macrofossils in Canadian Peatlands*. Ottawa: Agriculture Canada, Land Resource Research Centre, Research Branch.
- Loisel, J., and Garneau, M., 2010: Late Holocene paleoecohydrology and carbon accumulation estimates from two boreal peat bogs in eastern Canada: potential and limits of multi-proxy archives. *Palaeogeography, Palaeoclimatology, Palaeoecology*, 291(3): 493–533.
- Loisel, J., Gallego-Sala, A. V., and Yu, Z., 2012: Global-scale pattern of peatland *Sphagnum* growth driven by photosynthetically active radiation and growing season length. *Biogeosciences*, 9(84): 2169–2196.
- MacDonald, G. M., Beilman, D. W., Kremenetski, K. V., Sheng, Y., Smith, L. C., and Velichko, A. A., 2006: Rapid early development of circumarctic peatlands and atmospheric CH₄ and CO₂ variations. *Science*, 314(5797): 285–288.
- Makila, M., 1994: Calculation of the energy content of mires on the basis of peat properties. *Geological Survey of Finland, Report of Investigation*, 121: 1–73.
- Matsuura, K., and Willmott, C. J., 2009: Terrestrial Air Temperature and Precipitation: Monthly Climatologies, version 4.01 (1975–2005). <http://climate.geog.udel.edu/~climate/html_pages/Global2_Clim_README.global2_clim.html>, (accessed 4 September 2012).
- Moore, T. R., and Knowles, R., 1989: The influence of water table levels on methane and carbon dioxide emissions from peatland soils. *Canadian Journal of Soil Science*, 69(1): 33–38.
- Murray, K. J., Tenhunen, J. D., and Nowak, R. S., 1993: Photoinhibition as a control on photosynthesis and production of *Sphagnum* mosses. *Oecologia*, 96(2): 200–207.
- Olefelt, D., Roulet, N. T., Bergeron, O., Crill, P., Bäckstrand, K., and Christensen, T. R., 2012: Net carbon accumulation of a high-latitude permafrost palsa mire similar to permafrost-free peatlands. *Geophysical Research Letters*, 39(3): L03501, doi: <http://dx.doi.org/10.1029/2011GL050355>.
- Olsson, I. U., 1986: A study of errors in ¹⁴C dates of peat and sediment. *Radiocarbon*, 28(2A): 429–435.
- O'Reilly, B., 2011: *Paleoecological and Carbon Accumulation Dynamics of a Fen Peatland in the Hudson Bay Lowlands, Northern Ontario, from the Mid-Holocene to Present*. Master's thesis, Department of Geography, University of Toronto, Toronto, Canada, <https://tspace.library.utoronto.ca/bitstream/1807/31374/1/O'Reilly_Benjamin_C_201111_MSc_Thesis.pdf>.
- Ovenden, L., 1990: Peat accumulation in northern wetlands. *Quaternary Research*, 33(3): 377–386.
- Pachauri, R. K., and Reisinger, A., 2007: *Climate Change 2007: Synthesis Report. Contribution of Working Groups I, II and III to the Fourth Assessment Report of the Intergovernmental Panel on Climate Change*. Geneva: IPCC.
- Payette, S., Delwaide, A., Caccianiga, M., and Beauchemin, M., 2004: Accelerated thawing of subarctic peatland permafrost over the last 50 years. *Geophysical Research Letters*, 31(18): doi: <http://dx.doi.org/10.1029/2004GL020358>.
- Prentice, I. C., Sykes, M. T., and Cramer, W., 1993: A simulation model for the transient effects of climate change on forest landscapes. *Ecological Modelling*, 65(1): 51–70.
- R Development Core Team, 2012: *R: A Language and Environment for Statistical Computing*. Vienna, Austria: R Foundation for Statistical Computing. ISBN 3-900051-07-0, <<http://www.R-project.org/>>.
- Reimer, P. J., Baillie, M. G. L., Bard, E., Bayliss, A., Warren, B. J., Blackwell, P. G., Ramsey, C. B., Buck, C. E., Burr, G. S., Edwards, R. L., Friedrich, M., Grootes, P. M., Guilderson, T. P., Hajdas, I., Heaton, T. J., Hogg, A. G., Hughen, K. A., Kaiser, K. F., Kromer, B., McCormac, F. G., Manning, S. W., Reimer, R. W., Richards, D. A., Southon, J. R., Talamo, S., Turney, C. S. M., van der Plicht, J., and Weyhenmeyer, C. E., 2009: IntCal09 and Marine09 radiocarbon age calibration curves, 0–50,000 cal years BP. *Radiocarbon*, 51: 1111–1150.
- Riley, J. L., 2005: *Flora of the Hudson Bay Lowlands and Its Postglacial Origins*. Ottawa, Canada: National Research Council of Canada. ISBN 0-660-18941-0.
- Riley, J. L., 2011: *Wetlands of the Ontario Hudson Bay Lowland: a Regional Overview*. Toronto, Canada: Nature Conservancy of Canada.
- Riordan, B., Verbyla, D., and McGuire, A. D., 2006: Shrinking ponds in subarctic Alaska based on 1950–2002 remotely sensed images. *Journal of Geophysical Research–Biogeosciences*, 111(G4): doi: <http://dx.doi.org/10.1029/2005JG000150>.
- Roulet, N. T., 2000: Peatlands, carbon storage, greenhouse gases, and the Kyoto protocol: prospects and significance for Canada. *Wetlands*, 20(4): 605–615.
- Roulet, N. T., Jano, A., Kelly, A., Klinger, L. F., Moore, T. R., Protz, R., Ritter, J. A., and Rouse, W. R., 1994: Role of the Hudson Bay Lowland as a source of atmospheric methane. *Journal of Geophysical Research*, 99(D1): 1439–1454.
- Sannel, A. B. K., and Kuhry, P., 2009: Holocene peat growth and decay dynamics in sub-arctic peat plateaus, west-central Canada. *Boreas*, 38(1): 13–24.
- Sheng, Y., Smith, L. C., MacDonald, G. M., Kremenetski, K. V., Frey, K. E., Velichko, A. A., Lee, M., Beilman, D. W., and Dubinin, P., 2004: A high-resolution GIS-based inventory of the West Siberian peat carbon pool. *Global Biogeochemical Cycles*, 18(3): doi: <http://dx.doi.org/10.1029/2003GB002190>.
- Tarnocai, C., 2006: The effect of climate change on carbon in Canadian peatlands. *Global and planetary Change*, 53(4): 222–232.
- Tarnocai, C., Kettles, I. M., Lacelle, B., 2011: Geological Survey of Canada, Open File 6561. Ottawa: Natural Resources Canada, <<http://geoscan.nrcan.gc.ca/starweb/geoscan/servlet.starweb?path=geoscan/fulle.web&search1=R=288786#tphp>> (accessed 13 August 2012).
- Turetsky, M., Wieder, K., Halsey, L., and Vitt, D., 2002: Current disturbance and the diminishing peatland carbon sink. *Geophysical Research Letters*, 29(11): 21-1 to 21-4.
- Turetsky, M. R., Wieder, R. K., Vitt, D. H., Evans, R. J., and Scott, K. D., 2007: The disappearance of relict permafrost in boreal North America: effects on peatland carbon storage and fluxes. *Global Change Biology*, 13(9): 1922–1934.
- Turunen, J., Tomppo, E., Tolonen, K., and Reinikainen, A., 2002: Estimating carbon accumulation rates of undrained mires in Finland—Application to boreal and subarctic regions. *The Holocene*, 12(1): 69–80.
- van Bellen, S., Garneau, M., and Booth, R. K., 2011: Holocene carbon accumulation rates from three ombrotrophic peatlands in boreal Quebec, Canada: impact of climate-driven ecohydrological change. *The Holocene*, 21(8): 1217–1231.
- van Breemen, N., 1995: How *Sphagnum* bogs down other plants. *Trends in Ecology and Evolution*, 10(7): 270–275.
- Vitt, D. H., Halsey, L. A., Bauer, I. E., and Campbell, C., 2000a: Spatial and temporal trends in carbon storage of peatlands of continental western Canada through the Holocene. *Canadian Journal of Earth Sciences*, 37(5): 683–693.

- Vitt, D. H., Halsey, L. A., and Zoltai, S. C., 2000b: The changing landscape of Canada's western boreal forest: the current dynamics of permafrost. *Canadian Journal of Forest Research*, 30(2): 283–287.
- Waddington, J. M., Plach, J., Cagampan, J. P., Lucchese, M., and Strack, M., 2009: Reducing the carbon footprint of Canadian peat extraction and restoration. *AMBIO: a Journal of the Human Environment*, 38(4): 194–200.
- Wania, R., Ross, I., and Prentice, I. C., 2009a: Integrating peatlands and permafrost into a dynamic global vegetation model: 1. Evaluation and sensitivity of physical land surface processes. *Global Biogeochemical Cycles*, 23(3): GB3014, doi: <http://dx.doi.org/10.1029/2008GB003412>.
- Wania, R., Ross, I., and Prentice, I. C., 2009b: Integrating peatlands and permafrost into a dynamic global vegetation model: 2. Evaluation and sensitivity of vegetation and carbon cycle processes. *Global Biogeochemical Cycles*, 23(3): GB3014, doi: <http://dx.doi.org/10.1029/2008GB003413>.
- Webber, P. J., Richardson, J. W., and Andrews, J. T., 1970: Post-glacial uplift and substrate age at Cape Henrietta Maria, southeastern Hudson Bay, Canada. *Canadian Journal of Earth Sciences*, 7(2): 317–325.
- Yu, Z., Beilman, D. W., and Jones, M. C., 2009: Sensitivity of northern peatland carbon dynamics to Holocene climate change. In Baird, A. J., Belyea, L. R., Comas, X., Reeve, A. S., and Slater, L. D. (eds.), *Carbon Cycling in Northern Peatlands*. Washington, D.C.: American Geophysical Union, Geophysical Monograph Series, 184: 55–69.

MS accepted April 2013

APPENDIX

TABLE A1

¹⁴C samples, depth, ¹⁴C ages, and best-fit “Bacon” model calibration estimates for 17 previously published HBL-JBL cores.

Core	Depth (cm)	Lab I.D. #	Material	¹⁴ C age (BP)	±	Age range (cal yr BP)	Best fit (yr BP)
Albany	47–49	Beta-44532	Peat	1110	70	785–1245	1031
Albany	101–104	Beta-44534	Peat	2020	70	1720–2105	1922
Albany	155–160	Beta-44535	Peat	2450	90	2441–2876	2697
Albany	178–183	Beta-44533	Peat	2680	80	2744–3284	2946
Albany	210–215	Beta-44536	Peat	3750	70	3696–4266	4091
Albany	259–264	Beta-44537	Peat	4810	70	4983–5648	5386
Belec	37–40	Beta-53065	Peat	900	70	504–1174	888
Belec	50–52	Beta-53066	Peat	1350	60	1092–1427	1301
Belec	73–76	Beta-53068	Peat	2280	50	1898–2353	2339
Belec	95–100	Beta-54595	Peat	2770	70	2326–2851	2716
Belec	145–150	Beta-54596	Peat	3070	70	2992–3387	3262
Belec	195–200	Beta-54597	Peat	3430	11	3619–3869	3721
Belec	231–236	Beta-54598	Peat	3960	60	4132–4587	4302
EL1	12–13	Hela-1051	NA	2850	70	2781–3206	3033
EL1	98–99	Poz-19644	NA	4010	30	4314–4584	4483
EL1	136–138	Hela-1052	NA	4260	45	4792–5217	4948
EL1	180–186	Hela-1053	NA	5065	70	5590–5995	5659
Kuujjuarapik	0–1	UL-2367	NA	360	60	–151–1069	418
Kuujjuarapik	24–25	UL-2593	NA	1810	60	1549–1954	1773
Kuujjuarapik	54–55	UL-2592	NA	2900	70	2771–3216	2915
Kuujjuarapik	99–100	UL-2591	NA	3770	70	3673–4218	4036
Kuujjuarapik	154–155	UL-2590	NA	4080	100	4524–4949	4811
Kuujjuarapik	179–180	UL-2589	NA	4490	70	4976–5361	5171
Kuujjuarapik	209–210	UL-2587	NA	4850	70	5449–5804	5688
Kuujjuarapik	224–225	UL-2358	NA	5020	80	5694–6029	5889
LG2	44–45	Beta-199811	<i>Sphagnum</i> remains	1250	40	952–1482	1244
LG2	95–96	Beta-199812	<i>Sphagnum</i> remains	2500	40	2373–2713	2721
LG2	146–147	Beta-199813	<i>Sphagnum</i> remains	3350	40	3420–3670	3610
LG2	199–200	Beta-199814	<i>Sphagnum</i> remains	3830	40	4089–4379	4275
LG2	250–251	Beta-199815	<i>Sphagnum</i> remains	4210	50	4635–4915	4876
LG2	326–327	Beta-199816	<i>Sphagnum</i> remains	4960	50	5596–5911	5767
LG2	350–351	Beta-199817	<i>Sphagnum</i> remains	5300	50	5977–6282	6139
LG2	395–397	Beta-199819	Terrestrial plants macroremains	6100	40	6798–6891	6891
LG3	35–36	Beta-199818	<i>Sphagnum</i> remains	980	40	791–1271	932
LG3	75–76	Beta-199819	Terrestrial plants macroremains	2560	40	2374–2784	2749
LG3	130–131	Beta-199820	<i>Sphagnum</i> remains	3910	40	3802–4412	4281
LG3	190–191	Beta-199821	<i>Sphagnum</i> remains	4460	40	4881–5126	4959
LG3	249–250	Beta-199822	<i>Sphagnum</i> remains	4800	40	5411–5676	5542
LG3	329–330	Beta-199823	<i>Sphagnum</i> remains	5310	50	6111–6451	6187
LG3	374–375	Beta-180474	Terrestrial plants macroremains	5980	60	6715–7185	6835
LLC	51–52	UCI AMS 43480	<i>Sphagnum</i> stems	340	20	172–562	347
LLC	77–78	UCI AMS 58634	<i>Sphagnum</i> stems	915	15	773–913	885
LLC	102–103	UCI AMS 50203	<i>Sphagnum</i> stems	1205	15	1096–1276	1149
LLC	120–121	UCI AMS 57419	<i>Sphagnum</i> stems	1980	15	1882–1997	1919
LLC	140–141	UCI AMS 57421	<i>Sphagnum</i> stems	2550	15	2506–2771	2731

TABLE A1
Continued.

Core	Depth (cm)	Lab I.D. #	Material	¹⁴ C age (BP)	±	Age range (cal yr BP)	Best fit (yr BP)
LLC	153–154	UCI AMS 50204	<i>Sphagnum</i> stems	2915	15	2969–3154	3101
LLC	201–202	UCI AMS 43479	<i>Sphagnum</i> stems	3745	20	3988–4188	4010
LLC	250–251	UCI AMS 58636	<i>Sphagnum</i> stems	4165	20	4594–4844	4783
LLC	293–294	UCI AMS 50205	<i>Sphagnum</i> stems	4450	15	5008–5298	5076
LLC	350–351	UCI AMS 43478	<i>Sphagnum</i> stems	4985	20	5636–5921	5792
LLC	439–440	UCI AMS 50206	<i>Sphagnum</i> stems	6055	15	6817–7032	6879
LLC	480–483	Beta-223743	Ericaceous leaf fragments	6640	40	7431–7676	7576
Lost Moose	40–45	GSC-5321	Peat	290	80	308–678	448
Lost Moose	50–55	GSC-5226	Peat	420	90	450–1050	636
Lost Moose	68–73	GSC-5284	Peat	1990	70	1543–2118	1897
Lost Moose	125–135	GSC-5221	Peat	4270	70	4225–5250	4677
McClintock	18–20	Hela-670	Bulk peat	395	35	50–785	482
McClintock	70–72	AECV 1719C	Bulk peat	2230	80	2047–2732	2287
McClintock	108–110	Hela-3850	Bulk peat	4280	110	3992–5077	4616
McClintock	160–166	AECV 1718C	Wood	5810	90	6303–7098	6501
MOS	40–41	UCI AMS 57424	<i>Sphagnum</i> stems	355	15	168–678	452
MOS	70–71	UCI AMS 54958	<i>Sphagnum</i> stems	1270	25	1115–1305	1218
MOS	95–96	UCI AMS 64586	<i>Sphagnum</i> stems	1990	20	1863–2018	1927
MOS	108–109	UCI AMS 67515	<i>Sphagnum</i> stems	2065	25	2013–2148	2068
MOS	120–121	UCI AMS 54959	<i>Sphagnum</i> stems	2225	25	2177–2357	2164
MOS	136–137	UCI AMS 64588	<i>Sphagnum</i> stems	2490	20	2496–2746	2703
MOS	172–173	UCI AMS 54960	<i>Sphagnum</i> stems	3275	25	3396–3611	3553
MOS	224–225	UCI AMS 54961	<i>Sphagnum</i> stems	4185	25	4612–4882	4629
MOS	246–247	UCI AMS 57426	<i>Sphagnum</i> stems	4740	15	5289–5649	5437
MOS	296–297	Beta-223744	<i>Sphagnum</i> stems	6200	40	6709–7269	7049
MOS MaP1	60	UCI AMS 45796	<i>Sphagnum</i> stems, ericaceous leaves, and coniferous needles	925	20	676–1031	867
MOS MaP1	78	UCI AMS 45797	<i>Sphagnum</i> stems, ericaceous leaves, and coniferous needles	1280	20	1160–1300	1269
MOS MaP1	100–102	Beta-227710	<i>Sphagnum</i> stems, ericaceous leaves, and coniferous needles	2610	50	2214–2874	2610
MOS RiP2	42	UCI AMS 43471	<i>Sphagnum</i> stems	230	20	–182–868	309
MOS RiP2	56	UCI AMS 43470	<i>Sphagnum</i> stems, ericaceous leaves, and <i>Picea mariana</i> needles	1240	20	1099–1324	1272
MOS RiP2	69–71	UCI AMS 43472	Ericaceous leaves and coniferous needles	545	20	1489–2199	1633
MOS RiP2	75	UCI AMS 43473	<i>Picea mariana</i> needles	2350	100	1745–2460	2074
MOS RiP2	101–102	UCI AMS 50320	<i>Larix laricina</i> and <i>Picea mariana</i> needles	3040	15	3124–3524	3383
Oldman	33–36	Beta-44538	Peat	280	90	81–636	334
Oldman	45–48	Beta-44539	Peat	870	90	497–777	703
Oldman	63–66	Beta-44540	Peat	990	70	743–993	907
Oldman	69–74	Beta-43025	Peat	1010	70	819–1064	932
Oldman	97–102	Beta-43026	Peat	1520	70	1242–1517	1326
Oldman	134–144	Beta-42375	Peat	2010	70	1657–2092	1793
Oldman	158–163	Beta-43027	Peat	2940	70	1906–2321	2113
Oldman	200–205	Beta-42376	Peat	2610	70	2465–2850	2715

TABLE A1
Continued.

Core	Depth (cm)	Lab I.D. #	Material	¹⁴ C age (BP)	±	Age range (cal yr BP)	Best fit (yr BP)
Oldman	255–260	Beta-42377	Peat	3060	70	3165–3620	3446
Oldman	296	Beta-42378	Peat	3690	70	3894–4409	4212
Oldman	350–355	Beta-43028	Peat	4910	11	5426–5681	5594
Oldman	369–374	Beta-42379	Peat	5310	80	6124–6524	6255
Oldman	413–417	Beta-42380	Peat	5980	100	6453–6913	6517
Oldman	441–446	Beta-42381	Peat	5920	90	6811–7381	6908
Silcox	20–25	GSC-5265	Peat	550	50	495–685	542
Silcox	38–43	GSC-5266	Peat	1010	60	847–1302	993
Silcox	65–70	GSC-5245	Peat	3120	60	2688–3643	3359
SL1	1–2	Poz-19656	NA	115	0.36	–530–545	229
SL1	10–11	Poz-18597	NA	1120	30	833–1133	1042
SL1	41–42	Poz-16805	NA	1614	36	1445–1645	1559
SL1	45–46	Poz-10675	NA	1750	30	1563–1708	1658
SL1	58–59	Poz-19658	NA	1770	30	1716–1936	1834
SL1	66–67	Poz-19659	NA	2160	30	2002–2317	2278
SL1	83–84	Poz-16806	NA	2605	35	2566–2876	2784
SL1	91–92	Poz-19660	NA	2915	30	2907–3162	3027
SL1	114–115	Poz-19661	NA	3250	35	3397–3657	3567
SL1	124–126	AECV 1966c	NA	3690	90	3627–4027	3947
SL1	155–156	Poz-19662	NA	3890	35	4238–4848	4444
SL1	181.5–182.5	Poz-20142	NA	5250	40	5532–6217	5838
SL1	195–196	AECV 1905c	NA	5780	90	6181–6731	6406
STE	45–46	UCI AMS 54962	<i>Sphagnum</i> stems	105	30	–72–368	69
STE	67–68	UCI AMS 58645	<i>Picea</i> leaf fragments	600	20	559–669	650
STE	79–80	UCI AMS 64589	<i>Sphagnum</i> stems	1175	20	1001–1191	1078
STE	98–99	UCI AMS 54963	<i>Sphagnum</i> stems	1715	25	1552–1717	1641
STE	124–125	UCI AMS 65381	<i>Sphagnum</i> stems	2445	20	2345–2735	2399
STE	160–161	UCI AMS 54964	<i>Sphagnum</i> stems	3255	30	3356–3571	3512
STE	179–180	UCI AMS 67514	<i>Sphagnum</i> stems	3415	25	3608–3768	3703
STE	201–202	UCI AMS 65382	<i>Sphagnum</i> stems	3485	20	3777–3992	3853
STE	223–224	UCI AMS 54965	<i>Sphagnum</i> stems	3960	30	4183–4528	4287
STE	239–240	UCI AMS 58643	<i>Sphagnum</i> stems/ <i>Picea</i> leaf fragments	3975	15	4423–4863	4493
STE	285–286	UCI AMS 40360	<i>Sphagnum</i> stems	6225	20	5632–7302	5425
VC0406	62–63	Beta-281000	<i>Sphagnum</i> stems	1130	40	786–1286	1004
VC0406	110–111	Beta-281001	Twigs	2140	40	2010–2330	2153
VC0406	185–186	Beta-281002	<i>Sphagnum</i> stems	3770	40	3967–4392	4168
VC0406	237–238.5	Beta-280032	Wood	4760	40	5274–5649	5605
VC0406	303–304	Beta-281003	Wood fragments	5820	40	6580–6855	6729
VC0406	303–304	Beta-281004	Conifer needles	5890	40	6580–6855	6729

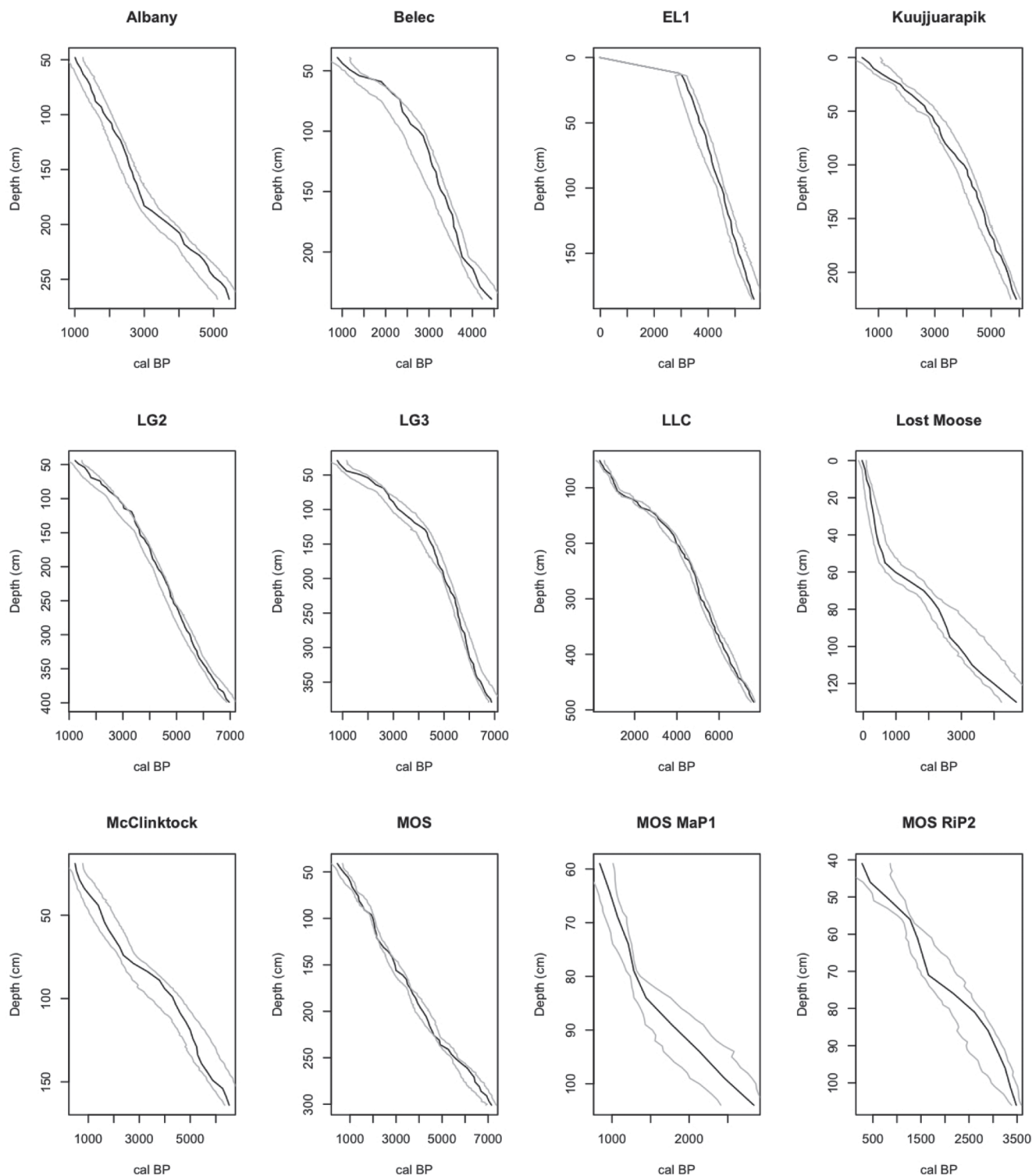


FIGURE 1A. “Bacon” age-depth models for 17 previously published peat cores. The best estimates for calibrated age (ybp) are shown in black. The upper and lower estimates are shown in gray.

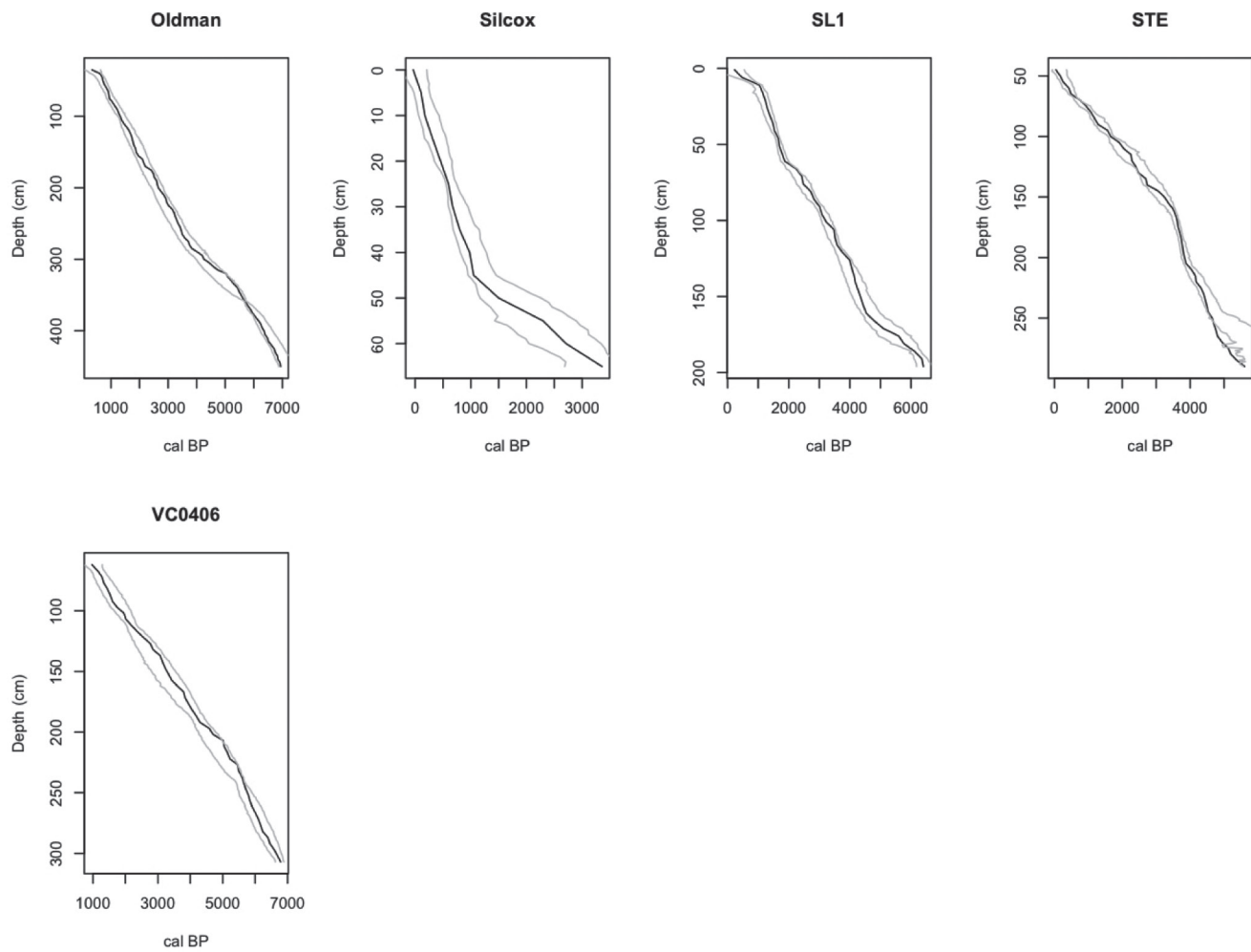


FIGURE 1A. (Continued.)